J. metamorphic Geol., 1999, **17**, 301–318

Origin and metamorphism of ultrabasic rocks associated with a subducted continental margin, Naxos (Cyclades, Greece)

Y. KATZIR,[1] D. AVIGAD,[1] A. MATTHEWS,[1] Z. GARFUNKEL[1] AND B. W. EVANS[2]
[1]*Institute of Earth Sciences, The Hebrew University of Jerusalem, Jerusalem 91904, Israel, (email: yaronk@vms.huji.ac.il)*
[2]*Department of Geological Sciences, University of Washington, Seattle, WA 98195-1310, USA*

ABSTRACT Meta-peridotites outcropping at different structural levels within the Alpine metamorphic complex of the Cycladic island of Naxos were studied to re-examine their metamorphic evolution and possible tectonic mechanisms for emplacement of mantle material into the continental crust. The continental margin section exposed on Naxos, consisting of pre-Alpine basement and *c.* 7 km thick Mesozoic platform cover, has undergone intense metamorphism of Alpine age, comprising an Eocene (M1) blueschist event strongly overprinted by a Miocene Barrovian-type event (M2). Structural concordance with the country rocks and metasomatic zonation at the contact with the felsic host rocks indicate that the meta-peridotites have experienced the M2 metamorphism. This conclusion is supported by the similarity between metamorphic temperatures of the ultrabasic rocks and those of the host rocks. Maximum temperatures of 730–760 °C were calculated for the upper-amphibolite facies meta-peridotites (Fo–En–Hbl–Chl–Spl), associated with sillimanite gneisses and migmatites. Relict phases in ultrabasics of different structural levels indicate two distinct pre-M2 histories: whereas the cover-associated horizons have been affected by low-grade serpentinization prior to metamorphism, the basement- associated meta-peridotites show no signs of serpentinization and instead preserve some of their original mantle assemblage. The geochemical affinities of the two groups are also different. The basement-associated meta-peridotites retain their original composition indicating derivation by fractional partial melting of primitive lherzolite, whereas serpentinization has led to almost complete Ca-loss in the second group. The cover-associated ultrabasics are interpreted as remnants of an ophiolite sequence obducted on the adjacent continental shelf early in the Alpine orogenesis. In contrast, the basement-associated meta-peridotites were tectonically interleaved with the Naxos section at great depth during the Alpine collision and high P/T metamorphism. Their emplacement at the base of the orogenic wedge is inferred to have involved isobaric cooling from temperatures of *c.* 1050 °C within the spinel lherzolite field to eclogite facies temperatures of *c.* 600 °C.

Key words: continental crust; meta-peridotites; Naxos; orogen.

INTRODUCTION

The most typical mode of occurrence of ultrabasic rocks in orogenic belts is in ophiolite sequences that represent ocean-derived material obducted onto continental margins or accreted above subduction zones (Moores, 1982; Nicolas, 1989). The ophiolite sequence is a rock association that resembles the oceanic lithosphere and is associated with deep-water sedimentary rocks. However, some high P/T orogenic belts contain rarer and more enigmatic ultrabasic associations, whereby peridotite lenses are enclosed within high-temperature leucocratic gneiss terranes derived from igneous and sedimentary continental protoliths. Such ultrabasic–upper continental crust associations occur in the Caledonian (Carswell, 1986; Jamtveit, 1987), Variscan (Medaris *et al.*, 1990; Kalt & Altherr, 1996; Schmädicke & Evans, 1997) and Alpine (Evans & Trommsdorff, 1978; Quick *et al.*, 1995) orogenic belts of Europe, and have been thoroughly studied because of their potential to reveal the composition of the subcontinental lithospheric mantle and the nature of mantle–crust interaction. A fundamental geodynamic question which has to be addressed is what kind of mechanism is responsible for emplacement of mantle rocks into the crust?

Intermingling of mantle-derived and surficial rocks requires large vertical movements, and may occur either by exhumation and denudation of the former or by burial of the latter. The occurrence of gneiss-enclosed ultrabasic rocks within eclogitic orogenic belts and the frequent similarity of the P–T peak conditions of the ultrabasics with those of the associated crustal eclogites indicate that the ultrabasic rocks and their continental hosts were involved in high P/T metamorphism. The initial juxtaposition of ultrabasic and upper crustal rocks could have taken place either at mantle depth during collision, or earlier in the orogenic history when the rocks were close to the Earth's surface. Juxtaposition at depth has been argued in several cases, mainly because most gneiss-enclosed ultrabasics were not serpentinized prior to high P/T

metamorphism (Schmädicke & Evans, 1997). In contrast to this, emplacement in the crust prior to subduction has been suggested in those cases where relicts of low-grade hydration assemblages were found in ultrabasic rocks (Evans & Trommsdorff, 1978). A possible scenario for such pre-orogenic shallow juxtaposition is the seafloor emplacement of subcontinental mantle during attenuation of passive continental margins (Boillot *et al*., 1988) and pre-oceanic rifts (Bohannon *et al*., 1989). Several of the large ultramafic masses of the Alps are thought to have been brought into the continental crust during such attenuation (Trommsdorff *et al*., 1993). It should be noted, however, that partial denudation and emplacement of a mantle diapir underneath thinned continental crust without serpentinization could be accomplished in a continental rift setting, as suggested for the Pyrenean lherzolites (Vielzeuf & Kornprobst, 1984) and the Ronda Peridotites (Davies *et al*., 1993; Tubia, 1994).

This paper focuses on ultrabasic bodies within the Alpine metamorphic complex of continental origin in the Cycladic island of Naxos (Fig. 1). The geological evolution of Naxos is dominated by a well-studied Miocene high-temperature Barrovian-type event (labelled M2) which overprinted and almost totally obliterated assemblages created during earlier Eocene high P/T metamorphism (M1) related to the collision of the Apulian and European plates. The ultrabasic rocks are located at different structural levels within the Naxos complex, ranging from the lowest-grade M2 rocks at high structural levels to upper amphibolite facies rocks adjacent to the leucogneiss core (Fig. 1). The field observations of Jansen (1977), amplified by our own detailed work in this study, show that the ultrabasic rocks were metamorphosed together with their host rocks during the M2 event, and that many of the ultrabasic rocks have undergone M2 metasomatic alteration. These intense deformation and crystallization fabrics mask those that developed in previous events, and make understanding of the mechanism of emplacement of ultrabasics in the continental section a challenging exercise. In this paper we present a study of the early (pre-M2) and M2 evolution of the Naxos metamorphic complex based on a detailed petrographic, petrological and geochemical analysis of the ultrabasic rock assemblages. This provides a new perspective on the P–T evolution on Naxos, and permits a re-examination of possible tectonic settings for emplacement of mantle material into the continental crust.

REGIONAL GEOLOGICAL SETTING

The Attic–Cycladic Massif (ACM) (Fig. 1) records a cycle of Alpine orogenic thickening, followed by extensional collapse in which low-angle detachments juxtaposed low-pressure metamorphic and unmetamorphosed rocks on top of exhumed high P/T units (Lister *et al*., 1984; Ridley, 1984; Avigad & Garfunkel, 1991; Gautier & Brun, 1994). The NW Cycladic high P/T sequence consists mainly of Mesozoic quartz-poor clastic and volcanic protoliths, probably representing a basic to intermediate volcanic province. The presence of some ophiolitic olistostromes and minor amounts of carbonates (Blake *et al*., 1981; Papanikolaou, 1987; Mukhin, 1996; Seck *et al*., 1996) within the sequence

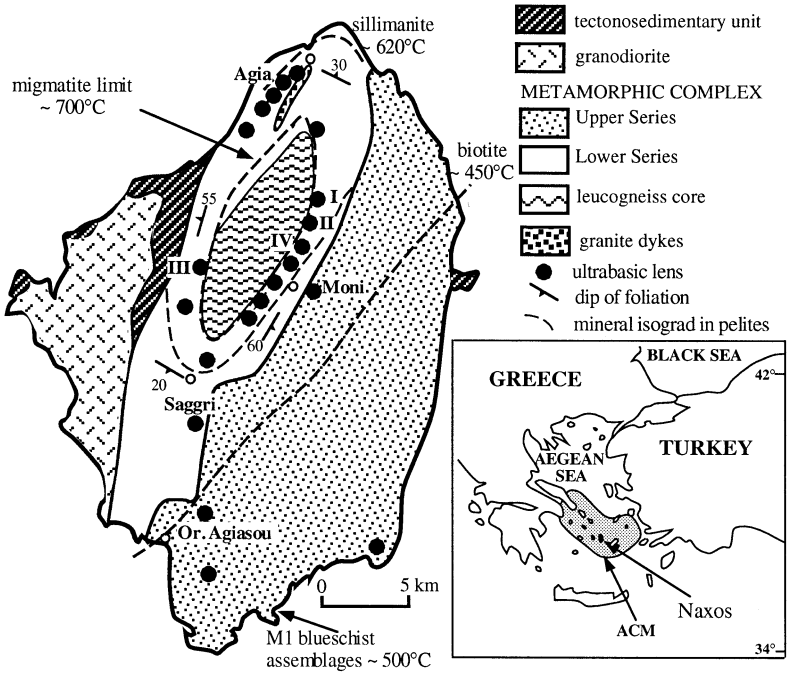

Fig. 1. A simplified geological map of Naxos after Jansen & Schuiling (1976) and Baker & Matthews (1994) showing the metamorphic complex (subdivided), the granodiorite and the tectono-sedimentary units. Ultrabasic rocks (in black) occur within the metamorphic dome at four different structural levels: (1) at the contact of the leucogneiss core with the overlying Lower Series (the 'main horizon') (roman numerals show the positions of the key outcrops which are described in the text); (2) Agia ultrabasics within the Lower Series; (3) at the contact between the Lower and Upper Units (outcrops near Saggri and Moni); and (4) within the Upper Series (Or. Agiasou). The M2 mineral isograds mapped by Jansen & Schuiling (1976) and modified by Feenstra (1985) and Buick (1988) are shown. ACM, Attic Cycladic Massif.

shows that an oceanic basin existed adjacent to this volcanic and clastic province, possibly placing it in an island arc terrane. In the central Cyclades (i.e. Naxos and Paros), the protoliths are of a continental origin, consisting of pre-Alpine granitic/quartzofeldspathic basement overlain by a Mesozoic sedimentary sequence dominated by shelf-carbonates (Dürr *et al*., 1978). Both these active and passive continental margin associations share a similar Tertiary metamorphic evolution, which includes an Eocene high P/T event (M1) followed by an Early Miocene low-P metamorphic overprint (M2) (Altherr *et al*., 1979; Andriessen *et al*., 1979; Schliestedt *et al*., 1987; Wijbrans & McDougall, 1988; Bröcker *et al*., 1993). The high-pressure metamorphic event is attributed to the closure of the Neo-Tethyan Pindos oceanic basin as a result of collision of the Apulian with the Pelagonian (European) microplates (Biju-Duval *et al*., 1977; Bonneau, 1984; Papanikolaou, 1987). The ultrabasic rocks studied in this paper thus occur within the continental part of the underthrusted Apulian microplate.

The metamorphic complex of Naxos forms an N–S elongated, thermal and structural dome (Fig. 1). The core of the dome is dominated by M2 migmatitic and meta-pelitic rocks ('leucogneiss core' of Buick, 1988), representing a reworked pre-Alpine basement (Andriessen *et al*., 1987; Keay & Lister, 1997; Reischmann, 1997). Overlying the leucogneiss core is a 7 km thick meta-sedimentary cover dominated by siliciclastic schists and gneisses in its lower part ('Lower Series' of Jansen & Schuiling, 1976), and by meta-bauxite bearing marble in its upper part ('Upper Series'). The grade of M2 metamorphism increases through a series of isograds from low-grade rocks still preserving M1 high-pressure assemblages to amphibolite facies rocks and partially molten migmatites at the core. Jansen & Schuiling (1976) estimated that M2 metamorphic conditions ranged from 400 °C and 5 kbar at the top of the sequence in SE Naxos to 700 °C and 7 kbar in the core. Textural observations and P–T estimates of metapelitic rafts within the core led Buick & Holland (1989) to argue that decompression from *c*. 8–6 kbar occurred whilst the rocks were undergoing M2 heating from 600 to 670 °C. Remnants of the older high P/T mineralogy have not been found in the leucogneiss core and the Lower Series. However, a recently reported occurrence of jadeite-bearing blueschist in SE Naxos indicates minimum pressures of 10–12 kbar and maximum temperature of 500 °C for the M1 event (Avigad, 1998), showing that decompression to M2 conditions involved cooling in SE Naxos. This contrasts with the prograde M2 heating in the core documented by Buick & Holland (1989).

Urai *et al*. (1990) and Buick (1991) suggested that M2 metamorphism took place during ductile extension in a shallowly northward-dipping crustal-scale shear zone. This extension continued during the intrusion of a post-metamorphic granodiorite at *c*. 12.1–13.6 Ma (Wijbrans & McDougall, 1988) along the western margin of the island (Fig. 1). Continued extension may also have been responsible for the tectonic emplacement of Tertiary unmetamorphosed sedimentary units onto both the granodiorite and the metamorphic complex (Jansen, 1977; Roesler, 1978; Lister *et al*., 1984; Lisker, 1993).

The ultrabasic rocks occur at four different stratigraphic and structural levels within the metamorphic sequence (Fig. 1): (1) within high-grade rocks at the boundary between the leucogneiss core and the Lower Series ('the main horizon'), (2) the Agia ultrabasic horizon within sillimanite grade rocks of the Lower Series, (3) within staurolite–kyanite grade rocks at the transition from the Lower Series to the Upper Series, and (4) within low-grade rocks of the Upper Series. The field evidence which suggests that the ultrabasic rocks experienced the M2 metamorphism includes their structural concordance with the country rocks and the well-developed metasomatic zonation at the contact with the felsic country rocks (Jansen, 1977). Jansen's (1977) petrographic studies also suggested that the metamorphic grade of the ultrabasics and of metasomatic zones increases towards the core in accordance with the M2 metamorphic grade in the country rocks. However, no detailed petrological analysis was presented in support of this pattern; such analysis is undertaken in this work.

ANALYTICAL METHODS

Mineral chemistry of representative rock samples was determined by a Jeol JXA 8600 electron microprobe at The Hebrew University of Jerusalem. Electron beam conditions were 15 keV and 10 nA. The results were corrected by the ZAF method. Whole-rock chemical analysis was carried out at the Geochemistry Division of the Geological Survey of Israel. Major and 3d transition element contents were determined by inductive coupled plasma atomic emission spectrometry (ICP–AES), and REE contents by inductive coupled plasma mass spectrometry (ICP–MS; Perkin Elmer SCIEX Elan 6000). For major and trace element ICP analysis, rock powders were digested by melting with $Li_2B_2O_4$ in platinum crucibles and with Na_2O_2 in zirconium crucibles, respectively. Loss on ignition (LOI) was determined by heating the sample at 1050 °C for 4 h and correcting for the oxygen weight added by the oxidation of Fe^{2+} to Fe^{3+}.

TEXTURAL AND MINERALOGICAL EVOLUTION OF THE ULTRABASIC ASSEMBLAGES

Main horizon of meta-ultrabasic bodies (leucogneiss core–Lower Series boundary)

The main and stratigraphically lowermost horizon of ultrabasic rocks (outcrops I–IV in Fig. 1) is composed of massive to moderately foliated, medium to coarse-grained meta-peridotites. Metasomatic monomineralic

zones are well developed at the contacts between the meta-peridotite bodies and the sillimanite gneiss country rock, usually in the order: gneisses, phlogopite, actinolite, anthophyllite (±talc), ultrabasic rocks (Jansen, 1977). In places the metasomatic process has completely obliterated the original metamorphic mineralogy of the peridotites. The petrographic and mineral compositional data that follow focus on four localities where relatively fresh and unaltered meta-peridotites survive: (I) west of Koronos Peak, (II) north of Keramoti village, (III) east of Kourounochorion village, and (IV) on the old cobbled path between the villages of Keramoti and Kinidharos (Fig. 1).

Representative microprobe analyses of minerals from the meta-peridotites are given in Table 1 and the petrography and mineral chemistry of these rocks are illustrated in Figs 2–5. Forsterite (Fo_{90-92}) is the dominant phase, with modal proportions ranging from 50–90%. Olivine forms a tabular polygonal mosaic (crystal size up to 2 mm), with a conspicuous preferred orientation, indicating syn-kinematic recrystallization of the ultramafic rock (Fig. 2a). Ca-amphibole (tremolite to Mg-hornblende, Fig. 3), enstatite (En_{90-93}, Fig. 4), and poikiloblastic chlorite, which is almost pure end-member clinochlore (Fig. 3), are all elongated in the same direction, defining the schistosity with the forsterite. Trails of grains of Cr–Al spinel, sometimes enclosed within chlorite, define pre-existing microfolded S-surfaces which are subparallel to the main schistosity. On the basis of the similarity between the metamorphic grade and structures of the ultrabasic rocks and the country rock, these deformation and crystallization fabrics, including the two schistosity generations, are considered to have developed in the meta-peridotites during M2 metamorphism.

The five-phase assemblage rock (Fo + En + Ca-Amph + Chl + Cr-spinel) is characteristic of meta-peridotite equilibrated under high amphibolite facies conditions (Trommsdorff & Evans, 1974; Evans, 1977). This paragenesis includes the equilibrium assemblage for the dehydration breakdown reaction of Mg-chlorite:

$$\text{clinochlore} \leftrightarrow \text{forsterite} + 2\ \text{enstatite} + \text{spinel} + 4\ H_2O \quad (1)$$

This univariant reaction in the MASH system was defined as an isograd in the Lepontine Alps within the sillimanite zone (isograd 7 of Trommsdorff & Evans, 1974). The similar location of the rocks on Naxos within the sillimanite zone is in agreement with this. There is limited textural evidence for the reaction being progressive, i.e. occurring from left to right in the sense of the equation above. First, in addition to the spinel, chlorite poikiloblasts contain neo-formed idiomorphic prisms of enstatite (Fig. 2b). Second, spinel is zoned from cores of opaque low Al-chromite to rims of translucent brown Al–Cr spinel (Fig. 5). This core-to-rim enrichment in Al and Mg and depletion in Cr and Fe^{2+} is indicative of a temperature increase within the high-amphibolite field (Evans & Frost, 1975; Frost, 1991).

Relics of an older, higher-grade meta-peridotite precursor to the M2 assemblages are well preserved in this horizon (Fig. 2c). Prisms of enstatite (3–4 mm) with prominent cleavage and more rare, large (5–6 mm) cracked crystals of forsterite are bent and kinked

Table 1. Electron microprobe analyses of representative minerals from Naxos ultrabasics.

	1 Opx	2 Opx	3 Opx	4 Opx	5 Ol*	6 Spl	7 Spl	8 Spl	9 Spl	10 Chl	11 Amp	12 Amp†	13 Amp	14 Amp
SiO_2	52.64	55.53	55.66	59.29	40.54	0.28	0.25	–	0.38	28.79	49.42	57.18	59.15	57.18
TiO_2	0.16	–	–	–	–	–	0.08	–	–	0.19	–	0.17	–	–
Al_2O_3	5.49	3.38	1.51	0.14	–	21.29	48.33	58.76	61.52	19.72	9.14	1.90	–	–
Cr_2O_3	–	–	–	–	–	42.82	17.37	9.25	3.77	1.14	–	0.31	–	–
FeO	7.68	7.68	6.02	6.01	10.25	21.55	13.41	11.18	12.23	2.55	2.38	2.09	8.00	13.71
MnO	0.23	–	–	–	–	–	0.26	–	–	0.14	0.15	0.22	0.29	0.68
MgO	33.27	34.20	34.77	37.18	48.37	9.38	17.30	19.60	20.01	33.44	24.26	24.09	31.17	25.53
CaO	0.90	0.13	0.10	0.07	–	0.20	0.09	0.10	0.08	–	12.49	13.15	0.41	0.28
Na_2O	0.17	–	0.01	0.06	–	–	–	–	–	–	0.07	–	0.07	0.02
Σ cations	100.5	100.9	98.07	102.8	99.16	95.52	97.09	98.89	97.99	85.97	97.91	99.11	99.09	97.40
Si	1.83	1.91	1.95	1.98	1.00	0.01	0.01	–	0.01	2.76	6.78	7.70	7.90	7.98
Ti	–	–	–	–	–	–	–	–	–	0.01	–	0.02	–	–
Al	0.23	0.14	0.06	0.01	–	0.82	1.58	1.80	1.88	2.23	1.48	0.30	–	–
Cr	–	–	–	–	–	1.11	0.38	0.19	0.08	0.09	–	0.03	–	–
Fe^{3+}	–	–	–	–	–	0.05	0.03	0.01	0.03	–	0.28	0.16	–	–
Fe^{2+}	0.22	0.22	0.18	0.17	0.21	0.54	0.29	0.24	0.24	0.20	–	0.07	0.89	1.60
Mn	–	–	–	–	–	–	0.01	–	–	0.01	0.02	0.03	0.03	0.08
Mg	1.72	1.75	1.82	1.86	1.78	0.46	0.71	0.76	0.77	4.78	4.96	4.83	6.21	5.31
Ca	0.03	0.01	–	–	–	0.01	–	–	–	–	1.84	1.90	0.06	0.04
Na	0.01	–	–	–	–	–	–	–	–	–	0.02	–	0.02	0.01
Sum	4.04	4.03	4.01	4.02	2.99	3.00	3.01	3.00	3.01	10.08	15.38	15.04	15.11	15.02

All values are wt%. * NiO (wt%) = 0.33; Ni (p.f.u.) = 0.006. † K_2O (wt%) = 0.01; K (p.f.u) = 0.002. Hyphens represent concentrations below the detection limit of the electron microprobe (<0.01 wt% or <0.01 cations p.f.u). All Fe was assumed to be divalent in pyroxene, olivine and chlorite. Fe^{3+} in spinel was calculated by stoichiometry. Fe^{3+} in amphibole was estimated according to the method of Leake *et al.* (1997). Samples 1 and 2, nk168/12, nk 168/32 (pre-M2 enstatite, Kourounochorion); sample 3, nk110B/8 (M2 enstatite, Koronos); sample 4, na193/7 (enstatite, Agia); sample 5, nk168/1 (pre-M2 olivine, Kourounochorion); samples 6 and 7, nk110/16c, nk110/17r (core and rim of M2 zoned spinel, Koronos); sample 8, nk122/44 (exsolution lamellae of spinel within pre-M2 enstatite, Keramoti); sample 9, nk169/13 (pre-M2 green spinel, Kourounochorion); sample 10, nk110/7 (chlorite, Koronos); sample 11, nk116/24 (hornblende, Koronos); sample 12, nk 169/7 (tremolite, Kourounochorion); sample 13, 93/12a (post-M2 anthophyllite, Agia); sample 14, ns145/ 67 (anthophyllite, Saggri).

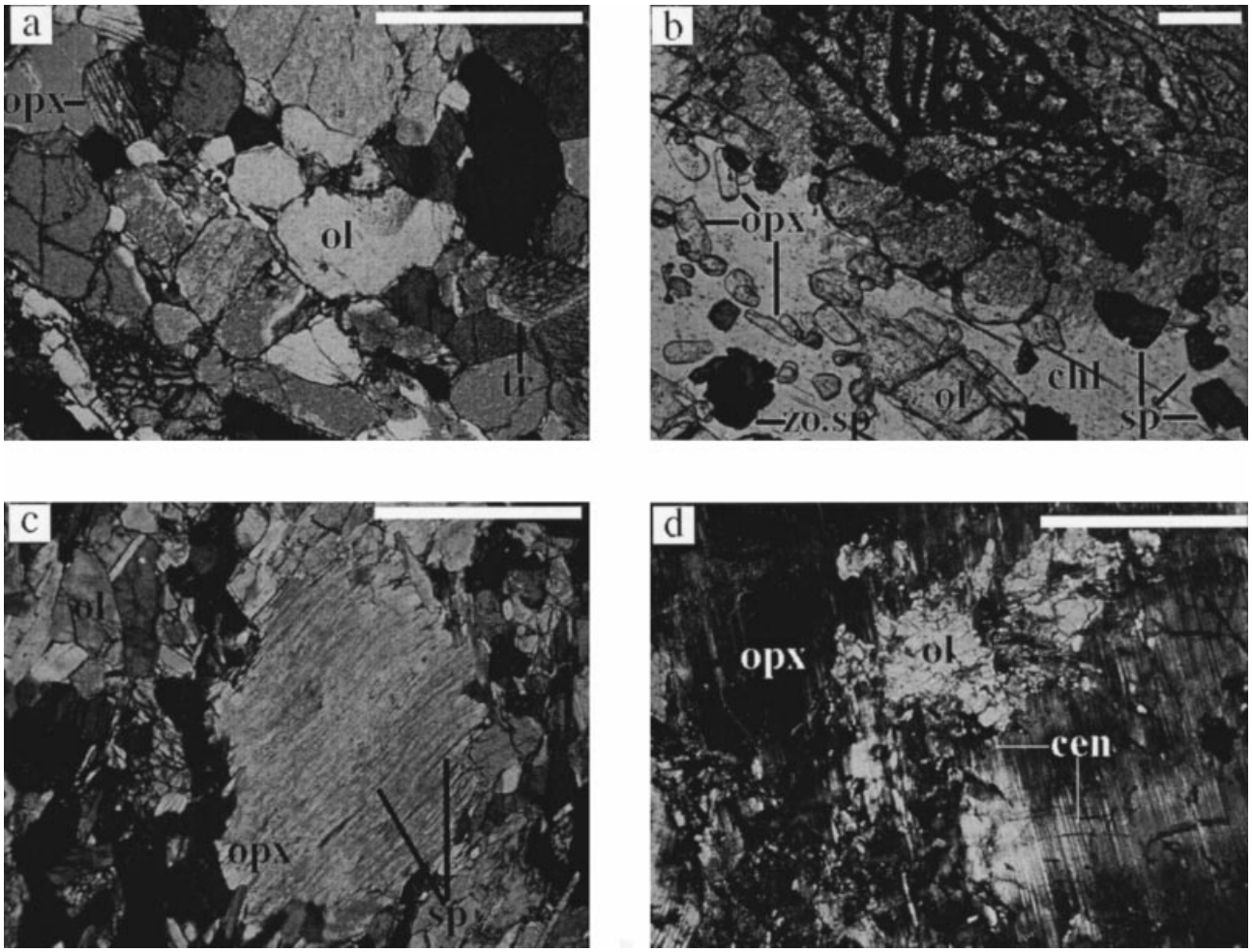

Fig. 2. Photomicrographs of thin sections of Naxos ultrabasic rocks: (a) M2 assemblage in Koronos meta-peridotite (XPL). The rock is dominated by large anhedral crystals of olivine, with orthopyropxene (low birefringent plate, prominent cleavage) and tremolite (basal section). Taken together, polygonal texture and preferred orientation are indicative of syn-kinematic crystallization. (b) M2 prograde reaction in Koronos meta-peridotite (PPL). Low-relief plate of chlorite is overgrown by neo-formed euhedral rods of orthopyroxene, olivine and zoned spinel. Spinel is zoned from dark Cr-rich cores to translucent Al-rich rims. (c) Pre-kinematic, deformed porphyroclast of orthopyroxene with exsolution lamellae of Cr-spinel set in M2-crystallized matrix (XPL, Kourounochorion meta-peridotite). (d) Relict olivine enclosed in a large porphyroblast of orthopyroxene with deformation lamellae of clinoenstatite (XPL, Agia ultrabasics). Abbreviations used: cen, clinoenstatite; chl, chlorite; ol, olivine; opx, orthopyroxene; sp, spinel; tr, tremolite; zo. sp, zoned spinel. Scale bars in photographs (a), (c), (d) = 1 mm; that in photograph (c) = 0.1 mm.

and possess a strong undulose extinction. The pre-kinematic enstatite contains aligned exsolution lamellae of Cr-spinel with the same compositional range as the brown Cr-spinel in the M2 groundmass (Fig. 5). These characteristics contrast with the enstatite crystals formed during M2, which are much smaller, undeformed, and lack exsolved spinel. In places, M2-enstatite rims have developed on crystals of earlier enstatite, which are identifiable by the undulose extinction and exsolution lamellae. The exsolution of spinel possibly occurred due to the decrease in solubility of Al and Cr in orthopyroxene during cooling, and would thus suggest that it formed at higher temperatures compared to those of the M2 event. Both generations of forsterite and enstatite have similar Mg-numbers (Fig. 4). However, whereas the neoformed M2 enstatite shows low Al_2O_3 contents (≤ 2 wt%), the relict pre-M2 enstatite has much higher Al_2O_3 contents of up to 5.5%. Rare grains of green spinel were found in the meta-peridotite at Kourounochorion. These crystals differ from the common brown granular spinel by their size (up to 0.5 mm); they are rimmed by retrograde magnetite, and have been altered to chromian chlorite. Morever, they are the most Al-rich of the spinels (60 wt% Al_2O_3, see Fig. 5). They are also interpreted as relics of the pre-M2 higher-grade peridotite.

Taken together, these petrographic and mineralogical relations suggest that mantle peridotites, formerly equilibrated in the spinel lherzolite field, cooled to at least high-amphibolite facies conditions and were incorporated into the Naxos continental section prior

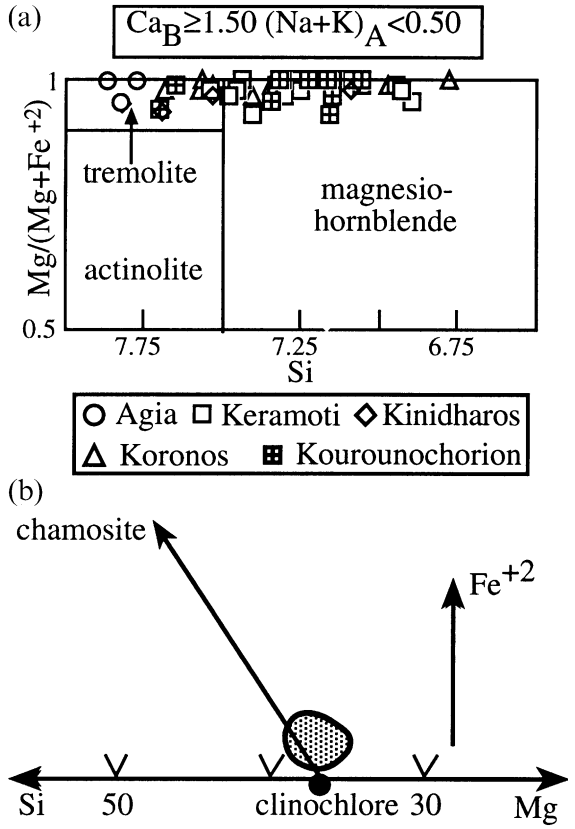

Fig. 3. (a) Electron microprobe analyses of amphibole from the main ultrabasic horizon and Agia, classified according to Leake *et al.* (1997). All amphibole is calcic: $Ca_B \leq 1.50$; $(Na+K)_A < 0.50$. Amphibole from the mono-mineralic metasomatic zones is not shown. (b) Electron microprobe analyses of chlorite from the main ultrabasic horizon and Agia plotted on a portion of the Fe–Mg–Si triangle (after Dalla Torre *et al.*, 1996). Chlorite from all localities plots on the solid solution line connecting the end-members clinochlore and chamosite, but very close to the clinochlore end-member (stippled area). The almost uniform composition of chlorite ($Mg_{4.8}Al_{2.4}Si_{2.8}O_{10}(OH)_8$) is similar to that of chlorite at its breakdown in ultrabasic rocks, to give spinel, olivine and orthopyroxene (Frost, 1975).

to the M2 event. They were then reheated and isofacially metamorphosed with the country rocks during M2.

Agia ultrabasics (NW Naxos)

A relatively continuous, 3 km long and 5–10 m thick ultrabasic horizon is exposed within sillimanite grade rocks of the Lower Series near the village of Agia, north of the leucogneiss core (Fig. 1). The country rocks are predominantly mafic biotite gneisses, interlayered with subordinate kyanite–sillimanite gneisses. Discontinuous metabasic lenses, consisting of fine-grained plagioclase, hornblende and epidote with a conspicuous preferred orientation, occur at the contact of the ultrabasic rock with biotite gneiss.

The ultrabasic rock at Agia is characterized by very coarse-grained, dark- and light-coloured domains, with no evidence of schistosity or of preferred orientation of the minerals. The dark domains consist of 2–3 cm long rectangular crystals of forsterite (Fo_{90-94}) whereas in the light parts, yellowish long prisms (up to 4 cm) of randomly oriented enstatite (En_{91-93}) occur within a fine-grained (100 μm) talc matrix. The enstatite frequently contains thin lamellae of clinoenstatite parallel to (100), as well as exsolution lamellae of spinel parallel to (010). Such clinoenstatite lamellae are induced by a shear transformation from enstatite ('stress mineral'), and are only known to occur in peridotites of the amphibolite facies (Trommsdorff & Wenk, 1968). Additional phases are anthophyllite, tremolite, chlorite and Al–Cr spinel. Microscopically, the idioblastic enstatite and talc appear to co-exist in excellent textural equilibrium. Such an equilibrium association of talc and enstatite is texturally quite different from that usually attributed to the commonly observed retrograde alteration and pseudomorphism of enstatite by talc. The stable paragenesis talc + enstatite has been shown experimentally to be on the high-P/low-T side of the reaction talc + 4 enstatite = anthophyllite (Greenwood, 1971; Chernosky *et al.*, 1985). However, there is no textural evidence in the Agia meta-peridotites to favour the crystallization of talc + enstatite at the expense of anthophyllite. Sprays of needles of clearly late anthophyllite ($Mg\text{-}Ath_{0.89}$) penetrate both olivine and neighbouring talc + orthopyroxene. Evans & Trommsdorff (1974) showed that the formation of enstatite + talc in amphibolite facies ultramafics of the Central Alps was caused by regional metamorphism accompanied by CO_2 metasomatism. However, in contrast to their assemblages, which contained large porphyroblasts of magnesite, the Agia ultrabasics contain no carbonate phase except for minor, probably late dolomite.

Petrography and field relations rather suggest that the talc + enstatite assemblage evolved at the expense of forsterite during the M2 event due to SiO_2 infiltration metasomatism, according to the reaction:

$$2 \text{ forsterite} + 3\ SiO_2\ (aq) + H_2O \leftrightarrow \text{enstatite} + \text{talc} \quad (2)$$

Silica-rich fluids penetrated the peridotite, formed the white domains, and left relict olivine, thus turning the peridotite into a variegated rock. Anthophyllite formation from talc + enstatite can occur either due to fall in pressure or an increase in Fe/Mg ratio of the system (Evans & Trommsdorff, 1974; Frost, 1975; Evans & Guggenheim, 1988). The high Mg content of post-M2 anthophyllite in Agia indicates that the system remained closed with respect to iron, thus favouring the first explanation. The interpretation that Si-metasomatism was responsible for the formation of the variegated rock is supported by the observation that relict olivine occurs as inclusions within enstatite or as xenomorphic relics within the talc matrix

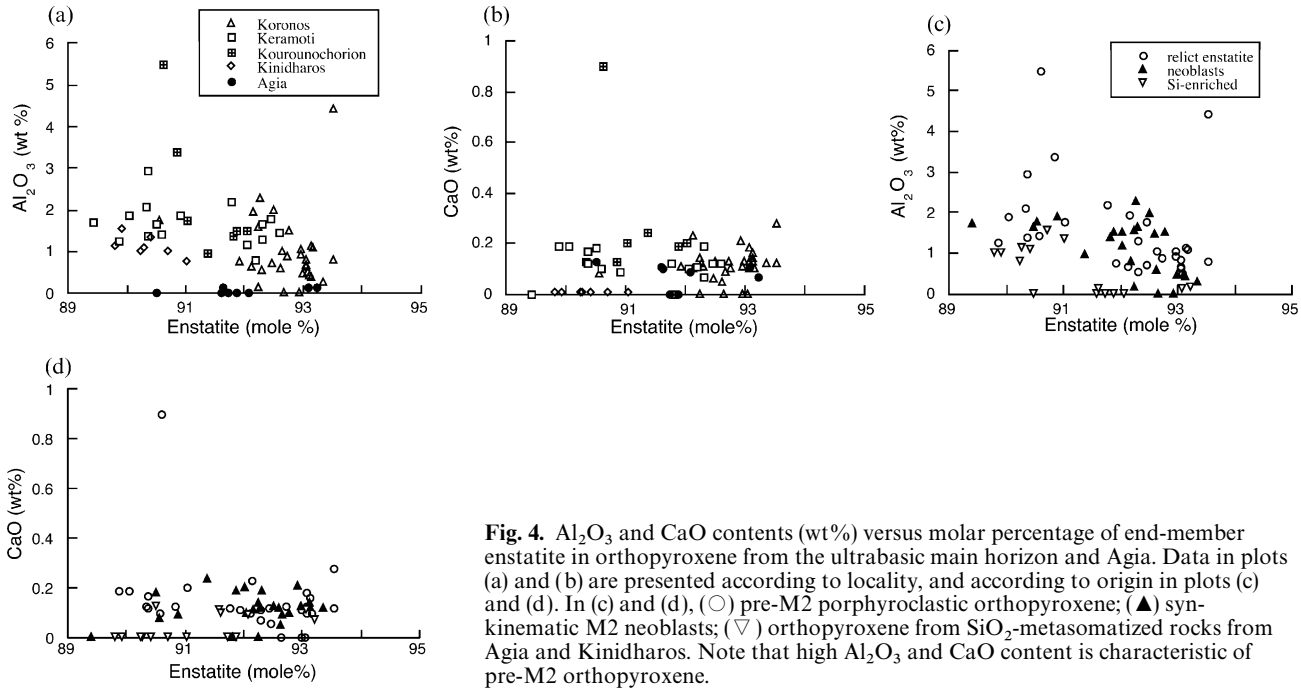

Fig. 4. Al_2O_3 and CaO contents (wt%) versus molar percentage of end-member enstatite in orthopyroxene from the ultrabasic main horizon and Agia. Data in plots (a) and (b) are presented according to locality, and according to origin in plots (c) and (d). In (c) and (d), (○) pre-M2 porphyroclastic orthopyroxene; (▲) syn-kinematic M2 neoblasts; (▽) orthopyroxene from SiO_2-metasomatized rocks from Agia and Kinidharos. Note that high Al_2O_3 and CaO content is characteristic of pre-M2 orthopyroxene.

(Fig. 2d). Oxygen isotope and petrological data suggest that this silica metasomatism occurred during the release of fluids from the crystallizing migmatites in the leucogneiss core at slightly post-peak M2 conditions (Baker & Matthews, 1994, 1995; Matthews *et al*., 1997; Katzir *et al*., unpublished data). Exsolved spinel within enstatite grains is observed, as in the peridotites of the main horizon, and indicates a high-T origin for the ultrabasics. Moreover, the presence of these lamellae also indicates that enstatite was present in the peridotite prior to the silica metasomatism. However, the Al-content of the Opx is low (Fig. 4), showing that it fully re-equilibrated at M2 conditions. In addition, poikiloblastic plates of chlorite enclosing neo-formed brown spinel and enstatite are observed, a prominent textural feature of prograde M2 metamorphism within the peridotite of the main horizon. Spinel is as aluminous as the rims of zoned spinel at Koronos and Keramoti (Fig. 5). Thus the assemblage that records the peak M2 conditions in Agia (Fo + En + Ca-Amph + Chl + Spl) is similar to that of the main horizon of ultrabasics.

Ultrabasic bodies within kyanite–staurolite grade rocks near the Lower Series–Upper Series boundary

These bodies are found at two sites, east of the village of Moni and south of the village of Saggri (Fig. 1).

Moni

The ultrabasic rocks at the Moni locality mainly consist of talc schists within kyanite–staurolite–garnet schists and garnet-bearing psammitic gneisses. The principal rock type is talc–anthophyllite schist with interlayers of talc–anthophyllite–magnesite phyllonite. Metasomatic zones of tremolite and chlorite are developed at the boundary with the pelitic country rock. The phyllonite consists of a sheared groundmass of fine-grained talc (70–80%), 2 mm long prisms of anthophyllite (10–20%), and 5 mm long porphyroclasts of brown-stained magnesite (10–20%). The absence of enstatite indicates a lower metamorphic grade than in the main ultrabasic horizon, in agreement with the metamorphic grade of the country rocks. The occurrence of magnesite in equilibrium with Mg-silicates indicates the presence of a CO_2-bearing fluid phase. The CO_2 possibly originated during decarbonation reactions in associated marbles, indicated by the crystallization of peak M2 calc-silicate assemblages (Baker *et al*., 1989; Baker & Matthews, 1994).

Saggri

At Saggri (Fig. 1), the ultrabasic rocks are exposed on a low hill in the middle of a cultivated plain and the field-relations with the country rocks are not well exposed. Massive blocks of gabbroic rocks, mostly metasomatized, jut out among poorly preserved soft ultrabasics. The latter are dominantly talc-magnesite rocks bordered by a very narrow anthophyllite zone and further away by chlorite and tremolite zones. As in Moni, the assemblage talc + magnesite suggests syn-metamorphic SiO_2-enrichment of the ultrabasic protolith and presence of a CO_2-bearing fluid phase. Rare and small pockets of dark green serpentinite are observed, consisting of very fine-grained antigorite and

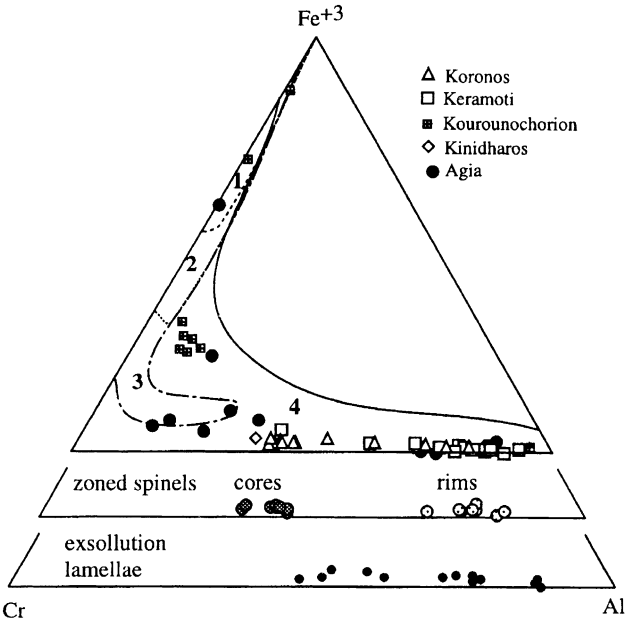

Fig. 5. Spinel compositions from the main ultrabasic horizon and Agia plotted on a Cr–Fe^{3+}–Al triangle. Compositional fields of spinel from (1) greenschist, (2) lower amphibolite, (3) medium amphibolite and (4) upper amphibolite facies ultrabasics are shown (after Evans & Frost, 1975; Frost, 1991; Mancini *et al*., 1996). The spinel with the highest Al content is a relict green spinel from the Kourounochorion meta-peridotite. Compositions of zoned spinels and of exsolution lamellae of spinel in pre-M2 orthopyroxene from the main ultrabasic horizon are shown on the attached lowermost portions of the triangle.

talc. The grade of this talc–antigorite assemblage ($T_{max} \leq 516$ °C; see below) is lower than that of the kyanite–staurolite country rocks, suggesting pre-M2 development of the serpentinite. This early low-grade assemblage is overgrown by fan-shaped bundles of 2.5 mm long prisms and fibres of anthophyllite (Mg-$Ath_{77–80}$) and idiomorphic plates (0.5 mm long) of talc.

Ultrabasic bodies within the Upper Series

Highly schistose serpentinite occurs as a continuous 1 km long, 5 m thick sheet NE of Ormos Agiasou (Fig. 1). It is associated with an intercalation of mica-schist within a sequence of medium-grained calcitic marbles. Metasomatic zones of chlorite and tremolite occur at the contacts with both schist and marble, and rounded fragments of yellow coarse-grained dolomitic marble (up to 20 cm long) are enclosed within the serpentinite. The ultrabasic assemblage consists of interpenetrating blades of antigorite (0.5 mm long), fine-grained talc and xenomorphic porphyroblasts of magnesite (1.5 mm long) elongated parallel to the schistosity. These syn-kinematic M2 phases overgrow an earlier fabric which is defined by a mesh of irregular veinlets of fine-grained magnetite. Such magnetite is considered to have been precipitated along grain boundaries of olivine in the ultrabasic precursor during low-temperature serpentinization (Vance & Dungan, 1977; Wicks & Whittaker, 1977). One cannot over-estimate the importance of this observation and the similar observation at Saggri since they indicate a stage of shallow equilibration in these ultrabasics prior to M2.

PETROLOGY AND THERMOBAROMETRY

The textural and mineralogical analysis given in the previous section shows that three phases of crystallization are observed in Naxos ultrabasic rocks. The dominant stage, observed in all three ultrabasic horizons, is syn-kinematic, increases in M2 grade towards the core of the dome and involves diffusion metasomatism. Relics of earlier crystallization events are preserved in the ultrabasic rocks indicating different histories: possible mantle equilibration for the main horizon and low-grade serpentinization for the Saggri and Or. Agiasou occurrences. A third stage of crystallization, mainly recorded in Agia ultrabasics, is shown to have been induced by infiltration metasomatism, probably associated with the M2 event.

Phase diagram calculations for M2 ultrabasics

The M2 (Fo + En + Hbl + Chl + Spl) paragenesis of the ultrabasics of the main horizon includes the equilibrium assemblage for the prograde breakdown reaction of Mg-chlorite. In this continuous reaction, chlorite first produces dark brown Al-poor chromite cores and then light-brown Al-rich chromite rims (Figs 2b & 5), together with enstatite, forsterite and H_2O. Univariant lines on a T–P_{H_2O} plot (Fig. 6) were calculated for Al-poorest and Al-richest spinel using THERMOCALC software version 2.5 (Holland & Powell, 1998) assuming $a_{H_2O} = 1$. Using the peak M2 pressure-estimate of 6 kbar for pelitic rafts within the leucogneiss core given by Buick & Holland (1989), a maximum temperature of 760 °C is given for the Al-richest spinel. If we correlate the core-to-rim change in spinel composition in ultrabasic assemblages with the 8→6 kbar decompression noted by Buick & Holland (1989), then a temperature increase of 680→760 °C is given (Fig. 7). These temperatures are higher than those previously suggested for M2 based on textural observations and geothermometry in the pelitic and granitic country rocks of the leucogneiss core. A minimum T-constraint for M2 is set by the destabilization of staurolite in the meta-pelite rafts by the reaction St + Ms + Qtz = Grt + Al-silicate + Bt + H_2O (Buick & Holland, 1989). Our calculation of this univariant reaction in the KFMASH system at pressures relevant to the pelites in the core yielded minimum temperatures of 640–650 °C (Fig. 7). This is consistent with the observation of some partial melting in the granitic/quartzofeldspathic rock types in the core, which requires $T > 650$ °C at 6 kbar, i.e. above

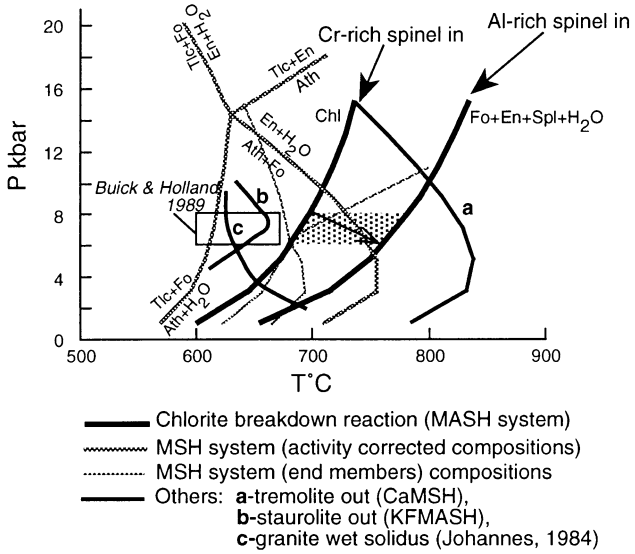

Fig. 6. Calculated T–P_{H_2O} equilibria for ultrabasic assemblages in the main horizon and Agia. M2 conditions for the main ultrabasic horizon are shown as a stippled region limited in temperature by the univariant lines for the breakdown dehydration reaction of chlorite. The arrow within the stippled region represents the progression of the M2 event, in which chlorite undergoes a continuous prograde reaction producing Al-poor spinel to Al-rich spinel, together with enstatite, forsterite and H_2O. Pressure limits for the M2 event are taken from Buick & Holland (1989) who suggested syn-heating decompression from 8 to 6 kbar during M2 (box). Equilibria for magnesian end-members of the minerals enstatite, forsterite, talc and anthophyllite in the MSH system are compared with the activity-corrected equilibria using mineral compositions from Agia Si-enriched peridotite. Also shown are univariant lines for the 'tremolite out' reaction (2 Fo + 2 Tr = 5 En + 4 Di + 2 H_2O) and the 'staurolite out' reaction (St + Ms + Qtz = Grt + Al-silicate + Bt + H_2O). The minimum granite melting curve is taken from Johannes (1984). Calculations are made using the software THERMOCALC version 2.5 (Holland & Powell, 1998).

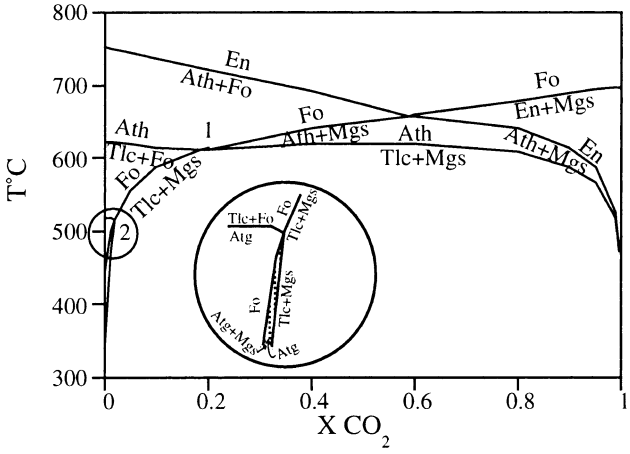

Fig. 7. T–X_{CO_2} grid at 6 kbar calculated using the mineral compositions of the ultrabasic assemblages at Moni and Or. Agiasou. The M2 Tlc–Ath–Mgs assemblage at Moni is stable along the univariant reaction line 2 Tlc + Mgs = Ath + CO_2 + H_2O. M2 conditions for Or. Agiasou are shown as a stippled region in the inset. Invariant point 1 [En, Atg] is located at T = 610 °C, X_{CO_2} = 0.19 and invariant point 2 [En, Ath] is located at T = 516 °C, X_{CO_2} = 0.02. Saggri mineral compositions give a slightly different topology to the diagram with the invariant points 1 and 2 converging to T, X_{CO_2} values of (541 °C, 0.04) and (509 °C, 0.018) respectively. Calculations are made using the THERMOCALC software version 2.5 (Holland & Powell, 1998).

the 'granite minimum melting curve' of Johannes (1984). At the maximum temperatures calculated in the ultrabasic rocks, 760 °C, fluid-absent biotite-dehydration melting reactions in metapelites should occur (Stevens *et al.*, 1997). These melting reactions are not observed in the highest-grade Naxos metapelites (I.S. Buick, personal communication), suggesting that temperatures were considerably lower than 760 °C. Moreover, textural relationships within the incipiently melted metapelitic gneisses are consistent with muscovite stability up to the point of anatexis, without the formation of alkali feldspar through muscovite dehydration reactions (Buick & Holland, 1991). M2 temperatures at the core were thus even lower than 720 °C, the temperature appropriate for muscovite dehydration melting at 6 kbar (Storré, 1977). Finally, based on the garnet–biotite exchange thermometer as calibrated by Hodges & Spear (1982), Buick & Holland (1989) calculated syn-M2 heating from 600 to 670 °C for metapelitic rafts within the leucogneiss core. Allowing for their stated uncertainty of ±50 °C and for possible resetting of the biotite, the peak M2 temperatures determined by Buick & Holland (1989) could be extended to 700 °C. Correspondingly, if we assume a slightly lower a_{H_2O} (e.g. 0.8), our calculated temperature in ultrabasics will drop by 30 °C and then overlap with the estimated peak M2 temperatures in meta-pelites. We thus believe that 700 °C is a reasonable estimate for peak M2 temperatures at Naxos leucogneiss core.

Figure 6 also compares the phase diagram for the reactions among the magnesian end-member minerals (Tlc, En, Fo, Ath) with the locations of the same equilibria using mineral compositions from Naxos peridotites. The 'enstatite + H_2O − in' reaction is shifted to higher temperatures, occurring at 750 °C at 6 kbar, in agreement with peak M2 temperatures calculated above for the ultrabasic rocks. The discrepancy between these temperatures and those estimated for the country rocks can be cleared up by assuming reduced a_{H_2O} = 1 in the calculation of the 'enstatite + H_2O in' reaction. The paragenesis talc + enstatite, found in SiO_2-enriched ultramafic rocks at Kinidharos and Agia, may potentially be used to define a lower pressure limit for M2 according to the reaction anthophyllite = talc + 4 enstatite. The use of this reaction as a barometer is hampered, however, by the large but imperfectly known effect of Fe (Evans & Trommsdorff, 1974; Frost, 1975; Evans & Guggenheim, 1988), and for example the assemblage talc + enstatite occurs in the Mount Stuart aureole, Central Cascades,

Washington, at pressures as low as 2 kbar (Frost, 1975). Thus, the very high pressures of greater than 14 kbar given by activity-corrected calculation of the above equilibrium should be taken as unreliable.

P–T determinations in the ultrabasics from higher stratigraphical levels are complicated by the fact that they have generally been exposed to infiltration metasomatism, resulting in rocks rich in talc and minerals such as anthophyllite and magnesite. The increase in modal talc during carbonation results from the increase in Si/Mg ratio of the silicate fraction of the rock due to the conversion of Mg-silicate to Mg-carbonate (Evans & Guggenheim, 1988). Figure 7 is a T–X_{CO_2} section in the CMSH system for equilibrium among the phases antigorite–talc–anthophyllite–forsterite–enstatite–magnesite, calculated for Moni and Or. Agiasou ultrabasics at 6 kbar. The M2 assemblage at Moni, talc–magnesite–anthophyllite, is stable only along the univariant reaction line $2\mathrm{Tlc} + \mathrm{Mgs} = \mathrm{Ath} + \mathrm{CO_2} + \mathrm{H_2O}$ confined to X_{CO_2} values higher than 0.19 and to temperatures of *c.* 580 °C except at very high X_{CO_2}. Petrological and stable isotope evidence indicates the existence of an H_2O-rich fluid phase ($X_{CO_2} \leq 0.3$) during M2 throughout most of the Lower Series (Baker *et al.*, 1989; Buick & Holland, 1991).

In the pure MSH system, the stable co-existence of anthophyllite with serpentine minerals is prevented by the talc + forsterite field. The introduction of CO_2 stabilizes anthophyllite + magnesite at lower temperatures than forsterite at $X_{CO_2} > 0.19$ (Fig. 7). This effect and the anomalously low Mg-content of anthophyllite ($X_{Mg} = 0.77$–0.80, relative to 0.89 at Agia and Moni) could account for its co-existence with antigorite at Saggri. Thus, on the T–X_{CO_2} section calculated using the mineral compositions of the ultrabasic assemblage at Saggri (not shown here), invariant points 1 [En, Atg] and 2 [En, Ath] converge to X_{CO_2}, temperature values of (0.038, 541 °C) and (0.0179, 509 °C) respectively. The relative high activity of Fe^{2+}, expressed in the anthophyllite composition, may be ascribed to the close proximity of meta-gabbroic rocks at Saggri.

The stable occurrence of antigorite with talc and magnesite at Or. Agiasou constrains the mole fraction of CO_2 to very low values (≤ 0.02) and sets the upper limit for temperatures at 516 °C (inset, Fig. 7).

Thermobarometry of pre-M2 high-temperature peridotite

The relics of high-temperature peridotite minerals preserved within the main ultrabasic horizon include aluminous enstatite, olivine and rare green spinel. Abundant Ca-amphibole in the M2 assemblage suggests that the precursor peridotite must have contained clinopyroxene as well, defining the protolith as lherzolite. Although temperatures in the spinel lherzolite field can be derived from the clinopyroxene–orthopyroxene solvus (Wood & Banno, 1973; Wells, 1977), the absence of relict clinopyroxene in the Naxos rocks requires thermometric methods based solely on orthopyroxene mineral chemistry, as follows.

Ca in orthopyroxene thermometer

Sachtleben & Seck (1981) first suggested this thermometer, and based their calibration on data in the CMS system at 15 kbar by Lindsley & Dixon (1976). Experimental work in the pyroxene quadrilateral (CFMS system) was summarized in a graphical thermometer by Lindsley (1983). Brey & Köhler (1990) re-calibrated the thermometer in the CMS system and showed it can be applied to natural systems, because Fe and Na have counter-balancing effects on the Ca content of Opx. The effect of pressure on the calculated temperature is small: 5 °C per 1 kbar in the pressure range of 5–20 kbar, according to the Brey & Köhler (1990) thermometer.

Al in orthopyroxene thermometer

Experimental studies in the MAS system (Fujii, 1976; Danckwerth & Newton, 1978; Gasparik & Newton, 1984) have shown that the solubility of Al in orthopyroxene co-existing with olivine and spinel is mainly a function of temperature. Addition of Ca and Fe to the system does not significantly change the temperature dependence of the equilibrium constant (Gasparik, 1984, 1987).

Most relict enstatite on Naxos was re-equilibrated during the M2 event, as indicated by their low CaO and Al_2O_3 contents, which are similar to those of the neo-formed M2 orthopyroxene, i.e. up to 0.25 and 2 wt% respectively (Fig. 4). To obtain the best temperature estimates for the pre-M2 phases, we chose the core of Opx no. NK168/12 (Table 1), which has the highest content of CaO and Al_2O_3 (0.90 & 5.49 wt% respectively). Equilibrium temperatures calculated by the three different versions of the 'Ca in Opx' thermometer at an assumed pressure of 15 kbar are in the range of 1025–1053 °C.

When applying the thermometer based on the experimental determination of Al-solubility in orthopyroxene to natural spinel lherzolite, one must make allowance for the fact that olivine rather than pure forsterite and a spinel of complex composition, rather than pure $MgAl_2O_4$, is present in natural rocks. The simplest approach is to regard all minerals as ideal ion-site solid solution (Stroh, 1976). The extended definition of the equilibrium constant thus becomes:

$$K = \frac{(x_{Fo}^{ol})^2 (x_{Al}^{M1})^{opx}}{(x_{Al}^{sp})^2 (x_{Mg}^{sp})(x_{Mg}^{M1})^{opx}} \qquad (3)$$

Within Naxos meta-peridotites, relict crystals of Opx, olivine and spinel are usually not in direct contact with each other, being surrounded by M2 groundmass. We thus applied the Gasparik & Newton

(1984) thermometer to relict crystals from two thin sections prepared from rock samples a few centimetres apart from a meta-peridotite at the Kourounochorion exposure: the core of Opx NK168/12, green spinel no. NK169/13 (Table 1) and olivine no. NK168/1. The temperature obtained, 1070 °C, is in good agreement with the Ca thermometer, suggesting that the relict assemblage in Kourounochorion represents equilibrium conditions. Several methods correcting for non-ideality of the Al–Cr mixing in the spinel phase have been suggested (Sachtleben & Seck, 1981; Sack, 1982; Webb & Wood, 1986). The Kouronochorion relict spinel is so aluminous ($Cr/(Cr+Al)=0.04$), however, that the effects of non-ideal mixing are negligible and temperatures calculated using these modifications are in the range of 1057–1070 °C.

Estimating the pressures at which relict spinel lherzolites equilibrated is much more difficult. At present, there is no reliable absolute barometer for spinel-bearing, garnet-free assemblages. The pressure can be constrained only by the experimentally determined stability field of natural spinel lherzolite. At 1050 °C, the lower and upper stability limits of spinel lherzolite, in which the orthopyroxene has an Fe-content of 10 mol%, are 8 and 14 kbar respectively (Gasparik, 1987). The transition from spinel lherzolite to garnet lherzolite is greatly influenced by the Cr content of the rock (O'Neill, 1981), and because Cr partitions strongly into spinel, increasing Cr content must extend its stability field to higher pressures. Furthermore, introducing Cr enables spinel and garnet to co-exist within a divariant *P–T* field, rather than along a univariant reaction curve. For high Cr values ($Cr/(Cr+Al)>0.2$), this field extends beyond 35 kbar (Nickel, 1986; Webb & Wood, 1986). However, assuming that the very low Cr value (0.04) of the relict spinel NK169/13 represents the Cr content of the protolith, the divariant field is very narrow and probably justifies 15 kbar as the upper limit.

MAJOR AND TRACE ELEMENT GEOCHEMISTRY

Representative major and trace element analyses, and calculated anhydrous spinel peridotite norms of Naxos ultrabasics are shown in Table 2. Meta-peridotites from the main horizon show substantial variability in normative mineral proportions, with samples ranging from lherzolites to harzburgites (2.8–9% diopside content) with some rare dunites. Spinel peridotite norms were recalculated to yield the three-phase peridotite triangle shown in Fig. 8. Ultrabasic rocks from the main horizon form a roughly linear trend, which is consistent with a depletion trend resulting from variable degrees of melting of similar source rocks, as observed within abyssal peridotites (Dick *et al*., 1984). We use major element variation diagrams with MgO as a fractionation index (Fig. 9). SiO_2, Al_2O_3 and CaO show negative linear correlations for the main horizon peridotites similar to those found in continental spinel lherzolite xenolith suites and ultramafic massifs and attributed to depletion processes caused by partial melt extraction (e.g. Frey & Green, 1974; Ringwood, 1975; McDonough, 1990; Becker, 1996). Samples with the lowest MgO contents are very close in composition to primitive upper mantle estimates (Jagoutz *et al*., 1979; Hart & Zindler, 1986; Hofmann, 1988).

Variations of Ni (compatible with olivine) and V (compatible with pyroxene) with MgO show that peridotites of the main horizon straddle both the harzburgite and lherzolite fields, and one sample shows dunitic characteristics (Fig. 10). The positive and negative correlations of Ni and V, respectively, with MgO in the main horizon peridotites are consistent with melt extraction.

Peridotites from the main horizon on Naxos show highly variable chondrite-normalized REE patterns (Fig. 11). However, only one sample (lherzolite NK124) shows flat HREE and sharp LREE depletion, indicative of a moderate amount (<10%) of fractional melting of 'primitive' spinel lherzolite (Johnson *et al*., 1990). The relatively flat patterns of the other samples suggest a later enrichment superimposed on an originally LREE-depleted pattern.

Analysed rocks from the Agia ultrabasics include samples from the less-metasomatized olivine-rich dark domain (NA193) and the talc–enstatite rich white domain (NA187). The normative mineralogies of these rocks resemble those of the main horizon, and their major and trace element compositions are close to the depletion trends defined by peridotites of the main horizon (Figs 8–10). This geochemical resemblence, which Si-metasomatism was not able to obscure, suggests a common origin for the Agia and main horizon ultrabasics.

The normative composition of Or. Agiasou serpentinite (NOA156) is harzburgitic (Fig. 8). This composition is meaningless for determination of the mantle protolith, because serpentinization involves complete loss of Ca and increase in the Si/Mg ratio of the former peridotite. The geochemical modification during serpentinization is well shown in the variation diagram (Fig. 9): the Or. Agiasou serpentinite is poorer in MgO, richer in SiO_2 and completely depleted in CaO relative to main horizon peridotites. The rather high Al_2O_3 content, comparable to that of the least depleted peridotites, might suggest a lherzolitic origin, since Al is rather conservative during serpentinization.

The talc–magnesite–anthophyllite rock from Moni (NMO226) plots within the olivine orthopyroxenite field in the normative triangle (Fig. 8), whereas the talc–enstatite rock from Kinidharos (NK75) and the talc–magnesite rock and talc serpentinite from Saggri (NS152, NS145) are quartz-normative (Table 2). The rather prominent, yet variable, SiO_2 enrichments and MgO depletions (Fig. 9) are explained by syn- to post-M2 metasomatism. Different origins, however, are indicated by the CaO contents: whereas rocks from

Table 2. Representative major, trace and rare earth element analyses and calculated anhydrous spinel peridotite norms of Naxos ultrabasics.

	nk 110	nk124	nk167	nk233	nk234	na187	na193	nm226	ns145	ns152	no156	nk 75
SiO_2	44.2	44.7	45.1	44.5	41.1	47.0	42.9	46.8	52.5	57.1	44.0	58.0
Al_2O_3	1.8	2.5	2.8	1.4	0.6	1.6	2.0	1.9	1.8	1.7	2.3	1.8
Fe_2O_3	8.5	9.0	8.8	10.0	10.5	8.5	8.4	6.3	8.0	6.5	9.5	8.0
TiO_2	<0.1	<0.1	<0.1	<0.1	<0.1	<0.1	<0.1	<0.1	<0.1	<0.1	0.1	<0.1
CaO	1.4	2.7	2.9	1.1	0.3	2.0	1.0	0.2	0.1	<0.1	0.2	1.7
MgO	42.0	36.5	37.5	44.0	45.5	39.5	40.0	31.0	29.5	28.5	32.2	27.0
MnO	0.12	0.12	0.12	0.12	0.12	0.07	0.1	<0.05	0.09	<0.05	<0.05	0.13
Na_2O	<0.02	0.1	0.1	<0.02	<0.02	<0.02	<0.02	<0.02	<0.02	<0.02	<0.02	0.04
K_2O	<0.02	<0.02	0.02	<0.02	<0.02	<0.02	<0.02	<0.02	<0.02	<0.02	<0.02	0.02
LOI	0.8	4.8	2.0	<0.1	0.5	1.3	3.9	13.1	6.8	5.2	9.9	3.5
Total	98.82	100.42	99.34	101.12	98.62	99.97	98.30	99.30	98.79	99.00	98.20	100.19
NORM												
Sp	1.58	2.54	2.76	1.15	0.46	1.54	1.87	2.84	–	–	2.90	–
Cpx	3.81	8.51	8.86	2.80	0.72	5.96	2.90	0.90	0.49	–	0.79	8.00
Opx	16.99	25.60	23.57	13.07	5.50	27.07	20.28	79.25	95.58	88.16	52.12	80.09
Ol	77.61	63.35	64.82	82.98	93.32	65.43	74.95	16.99	–	–	44.19	–
Qtx	–	–	–	–	–	–	–	–	3.93	11.84	–	11.91
ppm												
V	45	90	85	45	35	62	82	72	65	75	153	40
Cr	2700	3000	2850	3000	3200	3350	4670	2600	3350	4450	6500	850
Co	110	110	110	125	140	100	120	80	85	85	90	70
Ni	2300	2200	2200	2500	2900	1850	2600	1700	1700	2000	1800	1000
							C1					
La	0.1	0.1	0.5	0.4	0.3	0.5	0.31					
Ce	0.15	0.15	1.0	0.6	0.2	1.0	0.808					
Pr	0.02	0.03	0.1	0.1	0.07	0.1	0.122					
Nd	0.1	0.2	0.5	0.4	0.3	0.4	0.6					
Sm	0.06	0.1	0.2	0.1	0.1	0.1	0.195					
Eu	<0.02	0.04	0.06	0.03	<0.02	<0.02	0.074					
Gd	0.08	0.2	0.2	0.2	0.1	0.1	0.259					
Tb	<0.02	0.04	0.04	<0.02	<0.02	<0.02	0.047					
Dy	0.1	0.3	0.3	0.2	0.1	0.1	0.322					
Ho	<0.01	0.06	0.07	0.03	<0.01	0.03	0.072					
Er	0.06	0.2	0.2	0.1	0.06	0.08	0.21					
Tm	<0.01	0.03	0.04	0.02	<0.01	0.01	0.032					
Yb	0.1	0.2	0.3	0.2	0.1	0.1	0.209					
Lu	<0.01	0.04	0.04	0.03	<0.01	0.02	0.032					

Major and trace elements measured by ICP–AES analysis. REE measured by ICP–MS. nk110, Koronos peridotite; nk124, Keramoti Peridotite; nk167, Kourounochorion peridotite; nk233, nk234, Kinidharos peridotite; na187, na193, light and dark domains of Agia peridotite; nm226, Tlc–Ath–Mgs schist, Moni; ns145, Atg–Tlc–Ath serpentinite, Saggri; ns152, Tlc–Mgs schist, Saggri; no156, Or. Agiasou serpentinite; nk75, Tlc–En rock, Kinidharos. C1 Chondrite composition from Boynton (1984).

the Lower to Upper Series transition are strongly depleted in Ca (i.e. were previously serpentinized), those from the main horizon are not, hence were never even partially serpentinized.

It is clear that different processes have affected the chemical composition of Naxos ultrabasics. Variable degrees of melt extraction from a primitive spinel lherzolite are responsible for the geochemical variability of peridotites of the main horizon, including Agia. Unlike these peridotites, ultrabasic rocks from higher levels in the rock-column have suffered extensive low-temperature serpentinization. The geochemical trends thus match conclusions that we have drawn earlier from the study of the petrography and petrology of the rocks.

DISCUSSION

Ultrabasic rocks from three stratigraphic levels in the Naxos metamorphic complex were isofacially metamorphosed with their country rocks during the M2 event. In the context of the pre-M2 histories of the ultrabasic rocks, however, two major groups can be distinguished: rocks of the upper two ultrabasic horizons (Or. Agiasou, Saggri, Moni) were serpentinized at low temperatures prior to M2 metamorphism, whereas meta-peridotites associated with the leucogneiss core preserve evidence of a deep mantle equilibration event. This dissimilarity calls for different origins and modes of emplacement for the two distinct ultrabasic associations. It also suggests that the rock sequences hosting the ultrabasic rocks, i.e. the pre-Alpine basement and the Mesozoic sedimentary cover, do not represent an intact pre-metamorphic sequence, but were first juxtaposed during the Alpine orogeny in line with the geochronological evidence of Reischmann (1997).

The occurrence of early serpentinitic fabrics overprinted by M2 mineralogy and structures within the ultrabasics of the two upper horizons indicates that they were first denuded and hydrated at low temperatures during obduction and prior to Alpine metamorphism, most probably on the seafloor. This fact and their location in the section within the sedimentary

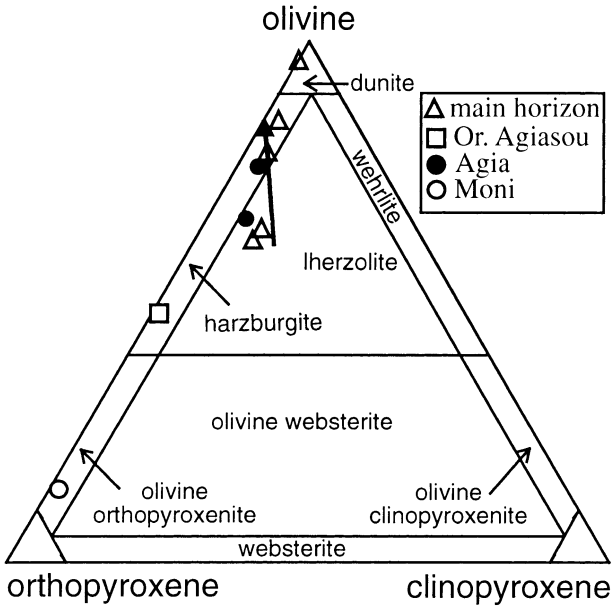

Fig. 8. Normative anhydrous composition of ultrabasics from Naxos. The arrow indicates the depletion trend resulting from variable degrees of melting of similar source rocks, as observed within abyssal peridotites (after Dick *et al.*, 1984).

shelf-type cover rather than in association with the basement, suggest a sub-oceanic origin for these ultrabasics. The Mesozoic continental shelf on which the shallow-water limestones and dolomites of the Upper Series of Naxos (Dürr *et al.*, 1978) were deposited, characterized by numerous events of exposure and erosion as indicated by the widespread occurrence of karst–bauxites, was thus adjacent to an oceanic basin. The serpentinites might have been incorporated into the crust prior to collision during the Eo-Hellenic event of ophiolite emplacement in the Early Cretaceous, which is well known on mainland Greece (Smith, 1993). The exact age of emplacement is, however, difficult to decipher since metamorphic recrystallization has left almost no paleontological evidence for the depositional age of the sedimentary precursors of the marbles, except for a Lower Cretaceous algae which occurs on the southern satellite island of Agrilos (Dürr *et al.*, 1978). The Mesozoic age assigned to the Naxotian marbles is mainly established by the correlation with unmetamorphosed bauxite-bearing carbonate sequences throughout the Mediterranean area (Feenstra, 1985). Nevertheless, straightforward correlation with any of the thick carbonate sequences of mainland Greece (Gavrovo–Tripolitza, Parnassos, Mount Olympus, Pelagonian; Robertson *et al.*, 1991) is not possible, since none contains associations of serpentinites and laterite-bearing karstic limestones as on Naxos (Feenstra, 1985).

The occurrence of ultrabasic rocks along major low-angle tectonic contacts in the Cycladic blueschist belt is not unique to Naxos (Papanikolaou, 1978; Avigad, 1993; Katzir *et al.*, 1996). However, the ultrabasic rocks of the NW Cyclades are associated with the crustal members of the oceanic lithosphere and are embedded within deep-water sedimentary sequences (Dixon & Ridley, 1987; Mukhin, 1996). They are thus thought to have been emplaced in the crust by upheaval of subducted fragments into an accretionary wedge during subduction of an oceanic plate. The setting we suggest here for the emplacement of the cover-associated ultrabasics of Naxos, obduction of ophiolites onto the continental margins prior to continental collision and high P/T metamorphism, is definitely different, but has been recognized in other parts of the Alpine belt (Avigad *et al.*, 1993 and references cited therein).

The potential to preserve pre-M2 relics is of special importance in the case of the main ultrabasic horizon at the contact of the leucogneiss core and the Lower Series, since no remnants of the Eocene high-pressure mineralogy were found within either of these sequences. Relict phases within the ultrabasics of the main horizon, including olivine, orthopyroxene and spinel, instead indicate pre-M2 equilibration in the spinel lherzolite stability field at granulite facies conditions. It is highly unlikely that the 1030–1070 °C temperatures determined by relict-orthopyroxene thermometry are representative of the Eocene high-P/T event, because they would imply large-scale melting of the whole sequence during M1. Ultrabasics of the main horizon were thus equilibrated at mantle depths prior to their incorporation to the Naxos continental sequence. The absence of preserved M1 relics in the ultrabasics

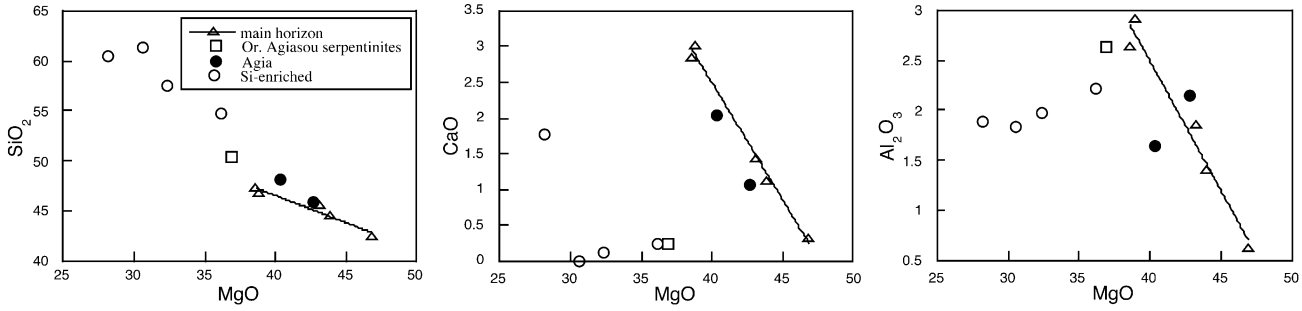

Fig. 9. Variation diagrams of SiO_2, Al_2O_3 and CaO versus MgO in Naxos ultrabasics. Open circles ('Si-enriched') refer to talc-dominated rocks from Moni, Saggri and Kinidharos.

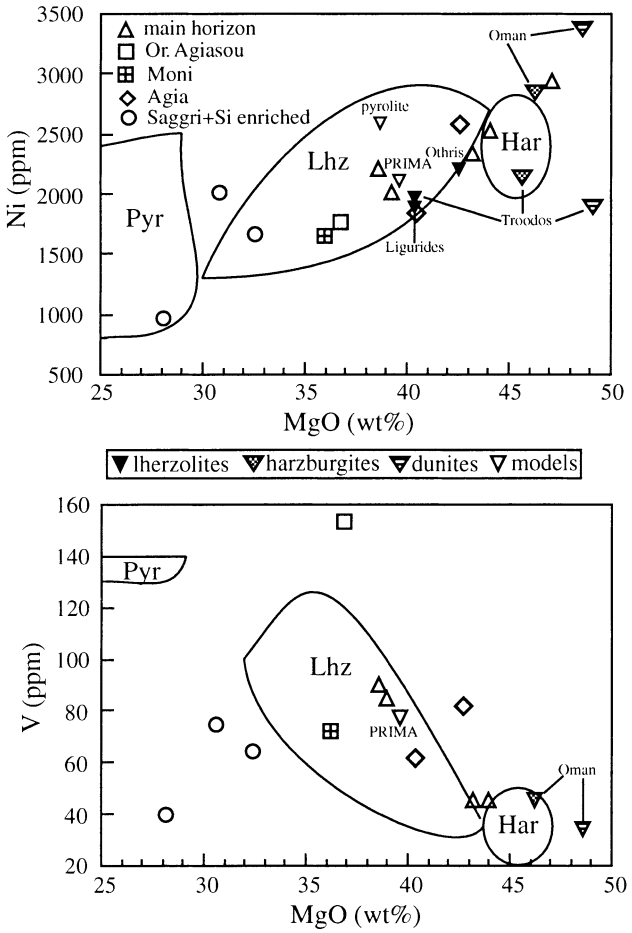

Fig. 10. Variation diagrams of Ni and V versus MgO in Naxos ultrabasics. Discriminative fields of harzburgite (har), lherzolite (lhz) and pyroxenite (pyr) from Pfeifer (1990). Data for Oman rocks are taken from Boudier & Coleman (1981), Troodos and Othris lherzolites from Menzies & Allen (1974), Troodos harzburgite and dunite from Coleman (1977), Lanzo lherzolite from Ottonello *et al.* (1984) and Liguride lherzolite from Ernst & Piccardo (1979). Pyrolite composition from Ringwood (1979) and PRIMA composition from Jagoutz *et al.* (1979).

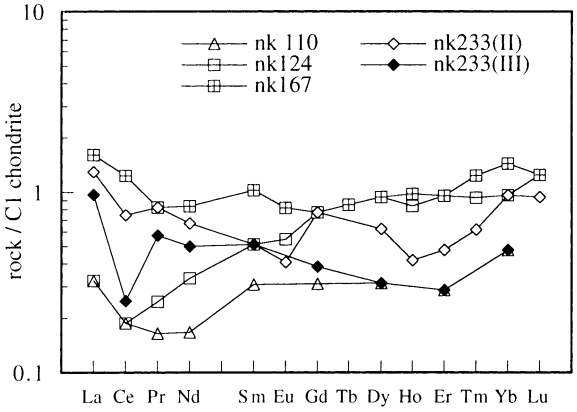

Fig. 11. Chondrite-normalized REE compositions of meta-peridotites from the main ultrabasic horizon on Naxos. nk110, Koronos harzburgite; nk124, Keramoti lherzolite; nk167, Kourounochorion lherzolite; nk233(II), Kinidharos harzburgite; nk233(III), Kinidharos dunite.

indicates that either they were emplaced in the crust between M1 and M2 or that former M1 ultrabasic mineralogy was totally effaced during M2, as was argued for the country rocks. However, during the M1–M2 interval, the subducted rocks were decompressed and located at shallower crustal levels (Wijbrans & McDougall, 1988). It is thus much more reasonable to assume that the incorporation of the mantle rocks occurred while the crustal rocks were either at maximum depth during M1 or prior to it, rather than during exhumation. Therefore, two possible scenarios can be proposed for the emplacement of the ultrabasics of the main horizon within Naxos gneisses (Fig. 12): (1) ultrabasic rocks were brought into contact with rocks of the upper continental crust while the latter were underthrust and buried to great depths in the course of the Alpine orogeny, possibly during Eocene collision that lead to M1 metamorphism; and (2) the ultrabasic rocks represent subcontinental mantle first denuded during rifting of the future Neo-Tethys prior to the Alpine Orogeny (e.g. Bay of Galicia, Boillot *et al.*, 1988).

As noted in the introduction, emplacement of ultrabasic rocks on the seafloor naturally involves serpentinization, and the absence of mineralogical and geochemical evidence for pre-M2 serpentinization of the ultrabasics of the main horizon (especially the non-depletion in Ca) strongly supports their deep-seated emplacement during Alpine collision. The absence of M1 mineralogy in the ultrabasics despite preservation of older mantle relics still needs explanation. A close examination of the *P–T* conditions of M1 and those of the last mantle equilibration of the ultrabasics may resolve this apparent discrepancy (Fig. 12). M1 pressures of at least 12 kbar and temperatures of up to 500 °C (Avigad, 1998) were estimated at the top of the section on SE Naxos, corresponding to a regional average gradient of *c.* 15 °C km^{-1}. Assuming that the 7 km thick section separating SE Naxos from the leucogneiss core is an intact M1 section, minimum pressures of *c.* 14 kbar and temperatures of 600 °C may be estimated for M1 at the core (Avigad, 1998). The maximum equilibration pressure of the spinel lherzolite prior to emplacement has been estimated at *c.* 15 kbar. Thus, the main effect of emplacement of mantle rocks in the crust during the M1 event would be isobaric cooling of the peridotites from $\geqslant$1000 °C to at least *c.* 600 °C, as indicated by cores of granular spinel. Such cooling would not cause any dramatic changes in the mineralogical assemblage of the ultrabasics, except for the possible stabilization of chlorite and amphibole, which are abundant in the M2 assemblage. It is thus concluded that on Naxos the peak-pressure conditions of crustal eclogites and spinel–peridotites and their subsequent exhumation

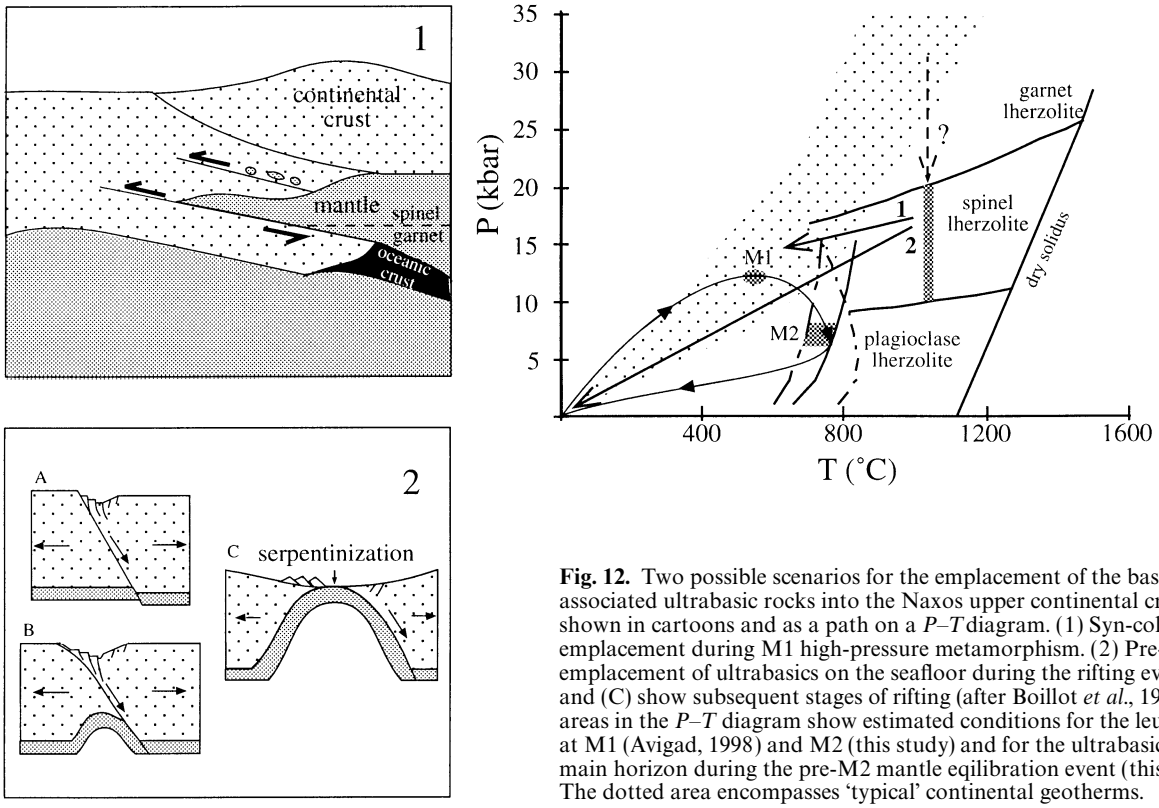

Fig. 12. Two possible scenarios for the emplacement of the basement-associated ultrabasic rocks into the Naxos upper continental crust section shown in cartoons and as a path on a *P–T* diagram. (1) Syn-collisional emplacement during M1 high-pressure metamorphism. (2) Pre-orogenic emplacement of ultrabasics on the seafloor during the rifting event. (A), (B) and (C) show subsequent stages of rifting (after Boillot *et al.*, 1988). Stippled areas in the *P–T* diagram show estimated conditions for the leucogneiss core at M1 (Avigad, 1998) and M2 (this study) and for the ultrabasic rocks of the main horizon during the pre-M2 mantle eqilibration event (this study). The dotted area encompasses 'typical' continental geotherms.

paths are compatible, as has been found in other gneiss-enclosed peridotites in high-P/T orogens. This observation and the lack of evidence for pre-metamorphic serpentinization of the ultrabasics indicate that mantle rocks were emplaced in the crustal section at depth during Alpine collision.

The 1050 °C temperatures at which the peridotites equilibrated are within the spinel stability field, and are well above typical continental geotherms (Fig. 12). This suggests that the rocks ascended from deeper levels in the mantle, yet had not cooled to the ambient geotherm before being emplaced in the crust. The geochemical trends of the ultrabasics of the main horizon show that the source rocks had experienced partial melting. The physical conditions derived for the last mantle equilibration of the ultrabasics are, however, well below the dry peridotite solidus (Fig. 12). The mantle equilibration event recorded in the ultrabasics thus post-dated melt extraction. It is impossible to further constrain the timing of melt extraction, yet one has to assume unrealistic departure from adiabatic trajectory in order to relate it to the ascent into the spinel stability field.

Summarizing the above discussion, the emplacement of the basement-associated peridotites from the subcontinental mantle into the continental crust was not a single, continuous event, but may be regarded as a two-step process. The thermal considerations suggest a stage of initial diapiric ascent into the spinel stability field. The diapirism ceased at depth of approximately 45–60 km, followed by the actual incorporation of the peridotites to subducted continental crust which involved almost isobaric cooling. Mantle diaprism is usually ascribed to lithospheric thinning in an extensional regime, whereas subduction of surface-derived rocks is naturally driven by compression. The time interval between cessation of extension and diapirism to the maximum thickening of the crust was short enough to mean that the peridotites avoided cooling to ambient temperatures while lingering in the upper mantle.

CONCLUSIONS

The Naxos metamorphic complex comprises two different ultrabasic sequences. The rocks of the structurally lower ultrabasic sequence, occurring close to the basement, were incorporated into the Naxos continental section at great depth, corresponding to the eclogite facies, during the Alpine orogeny. They were transported from the mantle directly into the orogenic wedge and they are therefore mantle flakes intermingled with the continental section during continental collision. In contrast, ultrabasic rocks of the higher structural levels appear to have been obducted onto the continental margins prior to the final closure of the Neo-Tethys ocean. They were serpentinized at shallow crustal levels and were later subducted and exhumed with the entire Naxos section.

ACKNOWLEDGEMENTS

This research was supported by a grant from the United States–Israel Bi-national Foundation to D. Avigad and B. W. Evans. Permission for field work in Greece was granted by the director of the IGME in Athens. We would like to thank the Geochemistry Division of the Geological Survey of Israel for the chemical analyses and S. Ehrlich and O. Yoffe for performing the analytical work. Thanks are also due to I. S. Buick and an unknown reviewer for critical reviews of the manuscript, which significantly contributed to its improvement.

REFERENCES

Altherr, R., Schliestedt, M., Okrusch, M., Seidel, E., Kreuzer, H., Harre, W., Lenz, H., Wendt, I. & Wagner, G. A., 1979. Geochronology of high pressure rocks on Sifnos (Cyclades, Greece). *Contributions to Mineralogy and Petrology*, **70,** 245–255.

Andriessen, P. A. M., Boelrijk, N. A. I. M., Hebeda, E. H., Priem, H. N. A., Verdurmen, E. A. Th. & Verschure, R. H., 1979. Dating the events of metamorphism and granitic magmatism in the Alpine orogen of Naxos (Naxos, Greece). *Contributions to Mineralogy and Petrology*, **69,** 215–225.

Andriessen, P. A. M., Banga, G. & Hebeda, E. H., 1987. Isotopic age study of pre-Alpine rocks in the basal units on Naxos, Sikinos and Ios, Greek Cyclades. *Geologie En Mijnbouw*, **66,** 3–14.

Avigad, D., 1993. Tectonic juxtaposition of blueschists and greenschists in Sifnos island (Greece) – implications for the structure of the Cycladic bluescist belt. *Journal of Strucrural Geology*, **15,** 1459–1469.

Avigad, D., 1998. High-pressure metamorphism and cooling on SE Naxos (Cyclades, Greece). *European Journal of Mineralogy*, **10**, 1309–1319.

Avigad, D. & Garfunkel, Z., 1991. Uplift and exhumation of high-pressure metamorphic terrains: the example of the Cycladic blueschist belt (Aegaen Sea). *Tectonophysics*, **188,** 357–372.

Avigad, D., Chopin, C., Goffé, B. & Michard, A., 1993. Tectonic model for the evolution of the western Alps. *Geology*, **21,** 659–662.

Baker, J. & Matthews, A., 1994. Textural and isotopic development of marble assemblages during the Barrovian-style M2 metamorphic event, Naxos, Greece. *Contributions to Mineralogy and Petrology*, **116,** 130–144.

Baker, J. & Matthews, A., 1995. The stable isotope evolution of a metamorphic complex, Naxos, Greece. *Contributions to Mineralogy and Petrology*, **120,** 391–403.

Baker, J., Bickle, M. J., Buick, I. S., Holland, T. J. B. & Matthews, A., 1989. Isotopic and petrological evidence for the infiltration of water-rich fluids during the Miocene M2 metamorphism on Naxos, Greece. *Geochimica et Cosmochimica Acta*, **53,** 2037–2050.

Becker, H., 1996. Geochemistry of garnet peridotite massifs from lower Austria and the composition of deep lithosphere beneath a Palaeozoic convergent plate margin. *Chemical Geoology*, **134,** 49–65.

Biju-Duval, B., Dercourt, J. & Le Pichon, X., 1977. From the Tethys ocean to the Mediterranean seas: a plate tectonic model of the evolution of the Western Alpine system. In: *Structural History of the Mediterranean Basins* (eds Biju-Duval, B. & Montadert, L.), pp. 143–164. Editions Technip, Paris.

Blake, M. C., Bonneau, M., Geyssant, J., Kienast, J. R., Lepvrier, C., Maluski, H. & Papanikolaou, D., 1981. A geologic reconnaissance of the Cycladic blueschist belt, Greece. *Geological Society of America Bulletin*, **192,** 247–254.

Bohannon, R. G., Naeser, C. W., Schmidt, D. L. & Zimmermann, R. A., 1989. The timing of uplift, volcanism and rifting peripheral to the Red Sea: a case for passive rifting? *Journal of Geophysical Research*, **94,** 1683–1701.

Boillot, G., Girardeau, J., Kornprobst, J., 1988. Rifting of the Galicia margin: crustal thinning and emplacement of mantle rocks on the seafloor. In: *Procceedings of the Ocean Drilling Program, Scientific Results, Volume 103* (eds Boillot, G., Winterer, E. L. *et al*.), pp. 741–756. College Station, Texas.

Bonneau, M., 1984. Correlation of the Hellenide nappes in the south-east Aegean and their tectonic reconstruction. In: *The Geological Evolution of the Eastern Mediterranean* (eds Dixon, J. E. & Robertson, A. H. F.), *Geological Society Special Publication,* **17,** 517–528. Blackwell, London.

Boudier, F. & Coleman, R. G., 1981. Cross section through the peridotite in the Samail ophiolite, southeastern Oman Mountains. *Journal of Geophysical Research*, **86,** 2753–2592.

Boynton, W. V., 1984. Geochemistry of the rare earth elements: meteorite studies. In: *Rare Earth Element Geochemistry* (ed. Henderson, P.), pp. 63–114. Elsevier, Amsterdam.

Brey, G. P. & Köhler, T., 1990. Geothermobarometry in four-phase lherzolites II. New thermobarometers, and practical assessment of existing thermobarometers. *Journal of Petrology*, **31,** 1353–1378.

Bröcker, M., Kreuzer, A., Matthews, A. & Okrusch, M., 1993. $^{40}Ar/^{39}Ar$ and oxygen isotope studies of poly-metamorphism from Tinos Island, Cycladic blueschist belt, Greece. *Journal of Metamorphic Geology*, **11,** 223–240.

Buick, I. S., 1988. *The metamorphic and structural evolution of the Barrovian overprint, Naxos, Cyclades, Greece*. PhD Thesis, University of Cambridge, Cambridge, UK.

Buick, I. S., 1991. The late Alpine evolution of an extensional shear zone, Naxos, Greece. *Journal of the Geological Society of London*, **148,** 93–103.

Buick, I. S. & Holland, T. J. B., 1989. The *P–T–t* path associated with crustal extension, Naxos, Cyclades, Greece. In: *Evolution of Metamorphic Belts* (eds Daly, J. S., Cliff, R. A. & Yardley, B. W. D.), *Geological Society Special Publication,* **43,** 365–369.

Buick, I. S. & Holland, T. J. B., 1991. The nature and distribution of fluids during amphibolite facies metamorphism, Naxos (Greece). *Journal of Metamorphic Geology*, **9,** 301–314.

Carswell, D. A., 1986. The metamorphic evolution of Mg–Cr type Norwegian garnet peridotites. *Lithos*, **19,** 279–297.

Chernosky, J. V., Day, H. W. & Caruso, L. J., 1985. Equilibria in the system $MgO–SiO_2–H_2O$: experimental determination of the stability of Mg-anthophyllite. *American Mineralogist*, **70,** 223–236.

Coleman, R. G., 1977. *Ophiolites, Ancient Oceanic Lithosphere?* Springer, New York.

Dalla Torre, M., De Capitani, C., Frey, M., Underwood, M. B., Mullis, J. & Cox, R., 1996. Very low-temperature metamorphism of shales from the Diablo Range, Franciscan Complex, California: new constraints on the exhumation path. *Geological Society of America Bulletin*, **108,** 578–601.

Danckwerth, P. A. & Newton, R. C., 1978. Experimental determination of the spinel peridotite to garnet peridotite reaction in the system $MgO–Al_2O_3–SiO_2$ in the range 900°–1100 °C and Al_2O_3 isopleths of enstatite in the spinel field. *Contributions to Mineralogy and Petrology*, **66,** 189–201.

Davies, G. R., Nixon, P. H., Pearson, D. G. & Obata, M., 1993. Tectonic implications of graphitized diamonds from the Ronda peridotite massif, southern Spain. *Geology*, **21,** 471–474.

Dick, H. J. B., Fisher, R. L. & Bryan, W. B., 1984. Mineralogic variability of the uppermost mantle along mid-ocean ridges. *Earth and Planetary Science Letters*, **69,** 88–106.

Dixon, J. E., & Ridley, J., 1987. Syros. In: *Chemical Transport in Metasomatic Processes*. NATO ASI Series (ed. Helgeson, H. C.), pp. 489–501. Reidel, Dordrecht.

Dürr, S., Altherr, R., Keller, J., Okrusch, M. & Seidel, E., 1978. The median Aegean crystalline belt: stratigraphy, structure, metamorphism, magmatism. In: *Alps, Appenines, Hellenides.*

Report 38 (eds Closs, H., Roeder, D. H. & Schmidt, K.), pp. 455–477. IUGS, Schweizerbart, Stuttgart.

Ernst, W. G. & Piccardo, G. B., 1979. Petrogenesis of some Ligurian peridotites – I. Mineral and bulk-rock chemistry. *Geochimica et Cosmochimica Acta*, **43,** 219–237.

Evans, B. W., 1977. Metamorphism of Alpine peridotite and serpentinite. *Annual Reviews in Earth and Planetary Science*, **5,** 397–447.

Evans, B. W. & Frost, B. R., 1975. Chrome-spinel in progressive metamorphism – a preliminary analysis. *Geochimica et Cosmochimica Acta*, **39,** 959–972.

Evans, B. W. & Guggenheim, S., 1988. Talc, pyrophyllite and related minerals. *Reviews in Mineralogy,* **19,** 225–294.

Evans, B. W. & Trommsdorff, V., 1974. Stability of enstatite + talc, and CO_2-metasomatism of metaperidotite, Val d'Efra, Lepontine Alps. *American Journal of Science*, **274,** 274–296.

Evans, B. W. & Trommsdorff, V., 1978. Petrogenesis of garnet lherzolite, Cima Di Gagnone, Lepontine Alps. *Earth and Planetary Science Letters*, **40,** 333–348.

Feenstra, A., 1985. *Metamorphism of bauxites on Naxos.* PhD Thesis, Rijksuniversiteit, Utrecht.

Frey, F. A. & Green, D. H., 1974. The mineralogy, geochemistry and origin of lherzolite inclusions in Victorian basanites. *Geochimica et Cosmochimica Acta*, **38,** 1023–1059.

Frost, B. R., 1975. Contact metamorphism of serpentinite, chloritic blackwall and rodingite at Paddy-Go-Easy Pass, Central Cascades, Washington. *Journal of Petrology*, **16,** 272–313.

Frost, B. R., 1991. Stability of oxide minerals in metamorphic rocks. *Reviews in Mineralogy,* **25,** 469–483.

Fujii, T., 1976. Solubility of Al_2O_3 in enstatite coexisting with forsterite and spinel. *Carnegie Institution of Washington Yearbook*, **75,** 566–571.

Gasparik, T., 1984. Two-pyroxene thermobarometry with new experimental data in the system $CaO–MgO–Al_2O_3–SiO_2$. *Contributions to Mineralogy and Petrology*, **87,** 87–97.

Gasparik, T., 1987. Orthopyroxene thermobarometry in simple and complex systems. *Contributions to Mineralogy and Petrology*, **96,** 357–370.

Gasparik, T. & Newton, R. C., 1984. The reversed alumina contents of orthopyroxene in the equilibrium with spinel and forsterite in the system $MgO–Al_2O_3–SiO_2$. *Contributions to Mineralogy and Petrology*, **85,** 186–196.

Gautier, P. & Brun, J. P., 1994. Crustal-scale geometry and kinematics of late-orogenic extension in the central Aegean (Cyclades and Evvia Island). *Tectonophysics*, **238,** 399–424.

Greenwood, H. J., 1971. Anthophyllite, corrections and comments on its stability. *American Journal of Science*, **270,** 151–154.

Hart, S. R. & Zindler, A., 1986. In search of a bulk-earth composition. *Chemical Geology,* **57,** 242–267.

Hodges, K. V. & Spear, F. S., 1982. Geothermometry, geobarometry and the Al_2SiO_5 triple point at Mt. Moosilauke, New Hampshire. *American Mineralogist*, **67,** 1118–1134.

Hofmann, A. W., 1988. Chemical differentiation of the earth: the relationship between mantle, continental crust and oceanic crust. *Earth and Planetary Science Letters*, **90,** 297–314.

Holland, T. J. B. & Powell, R., 1998. An internally consistent thermodynamic data set for phases of petrological interest. *Journal of Metamorphic Geology*, **16,** 309–343.

Jagoutz, E., Palme, H., Baddenhausen, H., Blum, K., Cendales, M., Dreibus, G., Spettel, E., Lorenz, V. & Wänke, H., 1979. The abundances of major, minor and trace elements in the earth's mantle as derived from primitive ultramafic nodules. In: *Early Solar System and Lunar Regolith. Proceedings of the 10th Conference on Lunar and Planetary Sciences, Volume 2.* (eds Merril, R. B., Bogard, D. D., Hoerz, F., McKay, D. S. & Robertson, P. C.), pp. 2031–2050. Pergamon, New York.

Jamtveit, B., 1987. Metamorphic evolution of the Eiksunddal eclogite complex, Western Norway, and some tectonic implications. *Contributions to Mineralogy and Petrology*, **95,** 82–99.

Jansen, J. B. H., 1977. *The Geology of Naxos. Geological and Geophysical Research No. 1.* Institute of Geological and Mining Research (IGME), Athens.

Jansen, J. B. H. & Schuiling, R. D., 1976. Metamorphism on Naxos: petrology and geothermal gradients. *American Journal of Science*, **276,** 1225–1253.

Johannes, 1984. Beginning of melting in the granite system $Qz–Or–Ab–An–H_2O$. *Contributions to Mineralogy and Petrology*, **86,** 264–273.

Johnson, K. T. M., Dick, H. J. B. & Shimizu, N., 1990. Melting in the oceanic upper mantle: an ion microprobe study of diopsides in abyssal peridotites. *Journal of Geophysical Research*, **95,** 2661–2678.

Kalt, A. & Altherr, R., 1996. Metamorphic evolution of garnet–spinel peridotites from the Variscan Schwarzwald (Germany). *Geologische Rundschau*, **85,** 211–224.

Katzir, Y., Matthews, A., Garfunkel, Z., Schliestedt, M. & Avigad, D., 1996. The tectono-metamorphic evolution of a dismembered ophiolite. *Geological Magazine*, **133,** 237–254.

Keay, S. & Lister, G., 1997. Inside the dome of the Naxos core complex. In: *Inside the Aegean Metamorphic Core Complexes. Technical Publication 44.* (eds Lister, G. & Forster, M.), pp. 75–87. Australian Crustal Research Centre, Monash University, Melbourne, Australia.

Leake, B. E., Woolley, A. R., Arps, C. E. S., Birch, W. D., Gilbert, M. C., Grice, J. D., Hawthorne, F. C., Kato, A., Kisch, H. J., Krivovichev, V. G., Linthout, K. *et al*., 1997. Nomenclature of amphiboles: reports of the subcommittee on amphiboles of the international mineralogical association, commission on new minerals and mineral names. *Canadian Mineralogist*, **35,** 219–246.

Lindsley, D. H., 1983. Pyroxene thermometry. *American Mineralogist*, **68,** 477–493.

Lindsley, D. H. & Dixon, S. A., 1976. Diopside–enstatite equilibria at 850°–1400°, 5–35 kbar. *American Journal of Science*, **276,** 1285–1301.

Lisker, S., 1993. *The tectonosedimentary upper units of the Cyclades.* MSc Thesis, The Hebrew University of Jerusalem.

Lister, G. S., Banga, G. & Feenstra, A., 1984. Metamorphic core complexes of Cordilleran type in the Cyclades, Aegean Sea, Greece. *Geology*, **12,** 221–225.

Mancini, F., Marshall, B. & Papunen, H., 1996. Petrography and metamorphism of the Sääksjärvi ultramafic body, southwest Finland. *Mineralogy and Petrology*, **56,** 185–208.

Matthews, A., Katzir, Y., Baker, J. & Avigad, D., 1997. Syn-metamorphic melting as a control of fluid release in the continental crust: a case study of the island of Naxos. *Terra Nova*, **9,** 204.

McDonough, W. F., 1990. Constraints on the composition of the continental lithospheric mantle. *Earth and Planetary Science Letters*, **101,** 1–18.

Medaris, L. G., Wang, H. F., Misar, Z. & Jel'nek, E., 1990. Thermobarometry, diffusion modelling and cooling rates of crustal garnet peridotites: two examples from the Moldanubian zone of the Bohemian Massif. *Lithos*, **25,** 189–202.

Menzies, M. & Allen, C., 1974. Plagioclase lherzolite—residual mantle relationships within two Eastern Mediterranean ophiolites. *Contributions to Mineralogy and Petrology*, **45,** 197–213.

Moores, E. J., 1982. Origin and emplacement of ophiolites. *Reviews in Geophysics and Space Physics*, **20,** 735–760.

Mukhin, P., 1996. The metamorphosed olistostromes and turbidites of Andros island, Greece, and their tectonic significance. *Geological Magazine*, **133,** 697–711.

Nickel, K. G., 1986. Phase equilibria in the system $SiO_2–MgO–Al_2O_3–CaO–Cr_2O_3$ (SMACCR) and their bearing on spinel/garnet lherzolite relationships. *Neues Jahrbuch Mineralogie Abhandlungen*, **155,** 259–287.

Nicolas, A., 1989. *Structures of Ophiolites and Dynamics of Oceanic Lithosphere.* Kluwer, Dordrecht.

O'Neill, HStC., 1981. The transition between spinel lherzolite and garnet lherzolite, and its use as a geobarometer. *Contributions to Mineralogy and Petrology*, **77,** 185–194.

Ottonello, G., Ernst, W. G. & Joron, L. J., 1984. Rare earth and 3d transition element geochemistry of peridotitic rocks: I. Peridotites from the Western Alps. *Journal of Petrology*, **25,** 343–372.

Palme, H. & Nickel, K. G., 1985. Ca/Al ratio and composition of the Earth's upper mantle. *Geochimica et Cosmochimica Acta*, **49,** 2123–2132.

Papanikolaou, D., 1978. Contribution to the geology of the Aegean Sea: the island of Andros. *Annales Géologiques des Pays Helléniques*, **29/2,** 477–553.

Papanikolaou, D., 1987. Tectonic evolution of the Cycladic blueschist belt (Aegean Sea, Greece). In: *Chemical Transport in Metasomatic Processes. NATO ASI Series* (ed. Helgeson, H. C.), pp. 429–450. Reidel Publishing Company, Dordrecht.

Pfeifer, H.-R., 1990. *Major and Trace Element Discrimination Diagrams to Determine Possible Protoliths of Orogenic Ultramafic Rocks*. Université de Lausanne.

Quick, J. E., Sinigoi, S. & Mayer, A., 1995. Emplacement of mantle peridotite in the lower continental crust, Ivrea–Verbano zone, northwest Italy. *Geology*, **23,** 739–742.

Reischmann, T., 1997. Single zircon Pb/Pb dating of tectonic units from the metamorphic complex of Naxos. *Greece. Terra Nova*, **9,** 496.

Ridley, J., 1984. Listric normal faulting and reconstruction of the synmetamorphic structural pile of the Cyclades. In: *The Geological Evolution of the Eastern Mediterranean* (eds Dixon, J. E. & Robertson, A. H. F.), *Geological Society Special Publication,* **17,** 755–762.

Ringwood, A. E., 1975. *Composition and Petrology of the Earth's Mantle*. McGraw-Hill, New York.

Ringwood, A. E., 1979. *Origin of the Earth and Moon*. Springer Verlag, New York.

Robertson, A. H. F., Clift, P. D., Degnan, P. J. & Jones, G., 1991. Palaeogeographic and palaeotectonic evolution of the Eastern Mediterranean Neotethys. *Palaeogeography, Palaeoclimatology, Palaeoecology*, **87,** 289–343.

Roesler, G., 1978. Relict of nonmetamorphic sediments on central Aegean islands. In: *Alps, Appenines, Hellenides. Report No. 38* (eds Cloos, H., Roeder, D. C. & Schmidt, K.), pp. 480–481. IUGS, Schweizerbart, Stuttgart.

Sachtleben, Th. & Seck, H. A., 1981. Chemical control of Al-solubility in orthopyroxene and its implications on pyroxene geothermometry. *Contributions to Mineralogy and Petrology*, **78,** 157–165.

Sack, R. O., 1982. Spinels as petrogenetic indicators: activity-composition relations at low pressure. *Contributions to Mineralogy and Petrology*, **81,** 169–186.

Schliestedt, M., Altherr, R. & Matthews, A., 1987. Evolution of the Cycladic crystalline complex: petrology, isotope geochemistry and geochronology. In: *Chemical Transport in Metasomatic Processes. NATO ASI Series* (ed. Helgeson, H. C.), pp. 389–428. Reidel Publishing Company, Dordrecht.

Schmädicke, E. & Evans, B. W., 1997. Garnet-bearing ultramafic rocks from the Erzgebirge, and their relation to other settings in the Bohemian Massif. *Contributions to Mineralogy and Petrology*, **127,** 57–74.

Seck, H. A., Koetz, J., Okrusch, M., Seidel, E. & Stosch, H. G., 1996. Geochemistry of a meta-ophiolite suite: an association of metagabbros, eclogites and glaucophanites on the Island of Syros, Greece. *European Journal of Mineralogy*, **8,** 607–623.

Smith, A. G., 1993. Tectonic significance of the Hellenic–Dinaric ophiolites. In: *Magmatic Processes and Plate Tectonics* (eds Prichard, H. M., Alabaster, T., Harris, N. B. W. & Neary, C. R.), *Geological Society Special Publication,* **76,** 213–243.

Stevens, G., Clemens, J. D. & Droop, G. T. R., 1997. Melt production during granulite facies anatexis: experimental data from 'primitive' metasedimentary protoliths. *Contributions to Mineralogy and Petrology,* **128,** 352–370.

Storré, B., 1977. Dry melting of muscovite + quartz in the range Ps = 7kb to Ps = 20kb. *Contributions to Mineralogy and Petrology*, **57,** 87–89.

Stroh, J. M., 1976. Solubility of alumina in orthopyroxene plus spinel as a geobarometer in complex systems: applications to spinel-bearing Alpine-type peridotites. *Contributions to Mineralogy and Petrology*, **54,** 173–188.

Trommsdorff, V. & Evans, B. W., 1974. Alpine metamorphism of peridotitic rocks. *Schweizerische Mineralogische und Petrographische Mitteilungen*, **54,** 333–352.

Trommsdorff, V. & Wenk, H. R., 1968. Terrestrial metamorphic clinoenstatite in kinks of bronzite crystals. *Contributions to Mineralogy and Petrology*, **19,** 158–168.

Trommsdorff, V., Piccardo, G. B. & Montrasio, A., 1993. From magmatism through metamorphism to sea floor emplacement of subcontinental Adria lithosphere during pre-Alpine rifting (Malenco, Italy). *Schweizerische Mineralogische und Petrographische Mitteilungen*, **73,** 191–203.

Tubia, J. M., 1994. The Ronda peridotites (Los Reals nappe): an example of the relationship between lithospheric thickening by oblique tectonics and late extensional deformation within the Betic Cordillera (Spain). *Tectonophysics*, **238,** 381–398.

Urai, J. L., Schuiling, R. D. & Jansen, J. B. H., 1990. Alpine deformation on Naxos (Greece). In: *Deformation Mechanisms, Rheology and Tectonics* (eds Knipe, R. J. & Rutter, E. H.), *Geological Society Special Publication,* **54,** 509–522.

Vance, J. A. & Dungan, M. A., 1977. Formation of peridotites by deserpentinization in the Darrington and Sultan areas, Cascade Mountains, Washington. *Geological Society of America Bulletin*, **88,** 1497–1508.

Vielzeuf, D. & Kornprobst, J., 1984. Crustal splitting and the emplacement of Pyrenean lherzolites and granulites. *Earth and Planetary Science Letters*, **67,** 87–96.

Webb, S. A. C. & Wood, B. J., 1986. Spinel–pyroxene–garnet relationships and their dependence on Cr/Al ratio. *Contributions to Mineralogy and Petrology*, **92,** 471–480.

Wells, P. R. A., 1977. Pyroxene thermometry in simple and complex systems. *Contributions to Mineralogy and Petrology*, **62,** 129–139.

Wicks, F. J. & Whittaker, E. J. W., 1977. Serpentine textures and serpentinization. *Canadian Mineralogist*, **15,** 459–488.

Wijbrans, J. R. & McDougall, I., 1988. Metamorphic evolution of the Attic Cycladic metamorphic belt on Naxos (Cyclades, Greece) utilizing $^{40}Ar/^{39}Ar$ age spectrum measurements. *Journal of Metamorphic Geology*, **6,** 571–594.

Wood, B. J. & Banno, S., 1973. Garnet–orthopyroxene and orthopyroxene–clinopyroxene relationships in simple and complex systems. *Contributions to Mineralogy and Petrology*, **42,** 109–124.

Received 25 April 1998; revision accepted 26 October 1998.